Excited state free energy calculation of fluorescence dye, Cy3 in different environments

Pilailuk Sawangsang

A Thesis Submitted in Partial Fulfillment of the Requirements for the
Degree of Master of Science in Physics
Prince of Songkla University
2014

Thesis Title	Excited state free energy calculation of fluorescence dye, Cy3 in different environments
Author	Miss Pilailuk Sawangsang
Major Program	Physics

Major Advisor

.....
(Dr.Chutintorn Punwong)

Co-advisor

.....
(Asst.Prof.Dr.Chittanon Buranachai)

Examining Committee

.....Chairperson
(Assoc.Prof.Dr.Teparksorn Pengpan)

.....
(Dr.Chalermpol Kanchanawarin)

.....
(Dr.Chutintorn Punwong)

.....
(Asst.Prof.Dr.Chittanon Buranachai)

The Graduate School, Prince of Songkla University, has approved this thesis as partial fulfillment of the requirements for the Degree of Master of Science in Physics

.....
(Assoc.Prof.Dr.Teerapol Srichana)
Dean of Graduate School

This is to certify that the work here submitted is the result of the candidate's own investigations. Due acknowledgement has been made of any assistance received.

.....Signature
(Dr.Chutintorn Punwong)
Major Advisor

.....Signature
(Pilailuk Sawangsang)
Candidate

ชื่อวิทยานิพนธ์ การคำนวณพลังงานเสรีในสถานะกระตุ้นของสารเรืองแสง Cy3 ในสภาวะต่างๆ
ผู้เขียน นางสาวพิไลลักษณ์ สว่างแสง
สาขาวิชา ฟิสิกส์
ปีการศึกษา 2557

บทคัดย่อ

Cyanine หรือ Cy3 เป็นสารเรืองแสง ที่มักจะมีการนำไปใช้โดยถูกติดไว้กับสารชีวโมเลกุล เพื่อใช้ในการสำรวจโครงสร้างและไดนามิกส์ โดยใช้กระบวนการเกิดฟลูออเรสเซนต์ (Fluorescence) ซึ่งสิ่งแวดล้อมที่ Cy3 อาศัยอยู่ มีผลต่อประสิทธิภาพของการเกิดฟลูออเรสเซนต์ และจะนำไปสู่คุณสมบัติทางโฟโตฟิสิกส์ที่แตกต่างกัน ประสิทธิภาพ (quantum yield) ของการเกิดฟลูออเรสเซนต์ของ Cy3 จะมีค่าต่ำมากในสารละลาย แต่จะเพิ่มขึ้นเมื่อสภาพแวดล้อมที่ Cy3 อยู่ทำให้โครงสร้างของ Cy3 มีความแข็งเกร็ง (rigid) เช่นการถูกติดไว้กับสายของดีเอ็นเอ ทั้งนี้กระบวนการเกิด ทราน-ซิส ไอโซเมอร์ไรเซชัน (Trans-cis isomerization) จะเป็นกระบวนการหลักที่แข่งกับกระบวนการเกิดฟลูออเรสเซนต์ โดยพบว่าค่ากำแพงศักย์ (energy barrier) ของการเกิด ทราน-ซิส ไอโซเมอร์ไรเซชัน ขึ้นกับสิ่งแวดล้อมที่ Cy3 อาศัยอยู่ งานวิจัยนี้ได้คำนวณหาค่ากำแพงศักย์ของ Cy3 ที่เป็นอิสระ (Free-Cy3), Cy3 ที่ติดกับสายเดี่ยวของดีเอ็นเอ (Cy3-ssDNA) และ Cy3 ที่ติดกับสายคู่ของดีเอ็นเอ (Cy3-dsDNA) ในเมทานอล โดยใช้ระเบียบวิธี QM/MM (Quantum mechanics/Molecular mechanics) โดยใช้ FOMO-CI (The semiempirical floating occupation molecular orbital configuration interaction) คำนวณในส่วนของปรากฏการณ์เชิงควอนตัม (QM) ส่วนสิ่งแวดล้อมจะคำนวณโดยใช้ระเบียบวิธี MM ค่าพลังงานงานอิสระ (Free energy) สามารถใช้บ่งบอกถึงกลไกเกี่ยวกับโฟโตไดนามิกส์ (Photodynamics) ที่จะเกิดขึ้นกับ Cy3 หรืออาจกล่าวได้ว่าความยากง่ายในการเกิดปรากฏการณ์ฟลูออเรสเซนต์และปรากฏการณ์ทราน-ซิส ไอโซเมอร์ไรเซชัน สามารถอธิบายได้จากค่าพลังงานอิสระ ซึ่งการหาค่าพลังงานอิสระ จะใช้ระเบียบวิธี Umbrella Sampling ร่วมกับระเบียบวิธี WHAM (The weighted histogram analysis method) จากการคำนวณพบว่า Cy3-dsDNA มีค่ากำแพงศักย์ของพลังงานอิสระมากที่สุด ส่วน Free-Cy3 และ Cy3-ssDNA จะให้ค่าที่ใกล้เคียงกัน ทั้งนี้เนื่องจาก Cy3-dsDNA มีอันตรกิริยาที่เกิดจากการซ้อนกัน (Stacking interaction) ของโครงสร้างวงแหวนที่มากกว่า ทั้งในส่วนของ Cy3 กับ primary strand และ Cy3 กับ complementary strand ของดีเอ็นเอสายคู่ จึงทำให้การหมุนของพันธะบริเวณคอนจูเกตเป็นไปได้ยากกว่า ส่งผลให้ค่ากำแพงศักย์ของ Cy3-dsDNA มีค่าที่สูงกว่า นอกจากนี้ ชนิดของเบสของดีเอ็นเอก็มีผลต่อปรากฏการณ์โฟโตฟิสิกส์

ของ Cy3 โดยเมื่อ Cy3 ติดกับไทมีน (Thymine; T) จะให้ค่ากำแพงศักย์ของการเกิด ทราน-ซิส ไอโซเมอร์ไรเซชัน มีค่าต่ำกว่าติดกับกวานีน (Guanine; G) อีกทั้งค่าของ steric hindrance ก็มีความเกี่ยวข้องกับการหมุนของพันธะบริเวณคอนจูเกตของ Cy3 โดยถ้า Cy3 มีค่า steric hindrance ที่สูง จะแสดงค่ากำแพงศักย์ของการเกิด ทราน-ซิส ไอโซเมอร์ไรเซชัน ที่สูงเช่นเดียวกัน ดังนั้นจึงเพิ่มประสิทธิภาพในการเกิดฟลูออเรสเซนต์

Thesis Title Excited state free energy calculation of fluorescence dye, Cy3 in different environments
Author Miss Pilailuk Sawangsang
Major Program Physics
Academic Year 2014

ABSTRACT

Cy3, a cyanine dye, is one of the most widely used fluorescence probe molecules in the investigation of the structure and dynamics of biomolecules by means of fluorescence methods. The effects of an environment on Cy3 are important in fluorescence applications and can lead to differences in its photophysical properties. The fluorescence quantum yields of Cy3 is very low in homogeneous solution but are considerably enhanced in the environment that rigidifies the structure, e.g. when it is attached to a DNA strand. A trans-cis isomerization of Cy3 is the main process that competes with fluorescence reaction and the efficiency of such process is reflected by the isomerization energy barrier which depends on Cy3's environment. In this work, the activation energies for isomerization of free Cy3, and Cy3 attached to a single- and double-stranded DNA in methanol are presented. The hybrid quantum mechanics/molecular mechanics (QM/MM) approach is employed to describe the quantum effects of Cy3 on the excited state while including the effects of environment with MM approach. The semiempirical floating occupation molecular orbital configuration interaction (FOMO-CI) method is used for electronic excited state calculations. The free energy calculations and subsequently the barrier for isomerization are performed by the umbrella sampling technique with the weighted histogram analysis method (WHAM). From the calculations, the activation energy of Cy3 attached to the double-stranded DNA is highest. However, when Cy3 is attached to the single-stranded DNA, its free energy barrier is similar to that of free Cy3. The stacking interaction to DNA is found to influence the photophysics of Cy3 by preventing the torsional rotation of Cy3's trimethine bridge. Unlike in ss-DNA, there is an additional stacking interaction presented in ds-DNA due to the complementary strand. Therefore it is more difficult to isomerize when Cy3 is attached to the ds-DNA. Furthermore, the type of DNA base

can also influence the stacking interaction which can also affect the photophysics of Cy3. If Cy3 is attached to the thymine (T) base of DNA rather than guanine (G), it shows the low energy barrier for trans-cis isomerization, thus decreasing the fluorescence efficiency. Moreover, the steric hindrance is associated with the rotation around the conjugated bonds of Cy3. If Cy3 has high steric hindrance, it shows the high energy barrier for the rotation, thus increasing the efficiency of fluorescence.

CONTENT

CONTENT (Continued)

LIST OF TABLES

LIST OF FIGURES

Page

Figure

CHAPTER 1

INTRODUCTION

1.1 Background and Rationale

Cy3 is among the oldest synthetic polymethine dyes that are widely used nowadays. It is a fluorescent dye that can show absorptions and emissions in the visible region to the infrared region.[1,2] It has been widely employed by attaching to DNA for investigating the structure and dynamics of nucleic acid. The properties of Cy3 strongly depend on its environment and can lead to differences in its photophysical properties. The fluorescence quantum yields of Cy3 is very low in homogeneous solution but are considerably enhanced in the environment that rigidifies the structure, e.g. when it is attached to a DNA strand.[3,4] After Cy3 molecule is activated to the electronic excited state, it immediately starts to relax via a couple of different deactivation mechanisms. There are two major decaying pathways from the excited state to the ground state. One is a radiative fluorescence process and the other is a nonradiative process by mean of isomerization or torsional rotation of the Cy3 molecule. A *trans-cis* isomerization of Cy3 competes with fluorescence reaction and the efficiency of such process is reflected by the isomerization energy barrier which depends on Cy3's environment. If the Cy3 dye has a rigid backbone which prevents the isomerization, that leads to a high energy barrier for the torsional motion. As a consequence, Cy3 will show the high fluorescence efficiency. The energy barrier for isomerization depends strongly on the rigidity of the Cy3 molecule enforced by the environment in which the dye is located. For example, when Cy3 can freely move in a solution, the torsional barrier is low and thus it shows low fluorescence quantum yield.[3,4] On the other hand when it is bonded to a DNA, the isomerization barrier becomes higher and the yield increases considerably.[3,4]

Therefore in this thesis, the calculations of the energy barrier for isomerization of Cy3 in different environments are performed so that the results can explain the efficiency of fluorescence and can be used as database of cyanine dyes for many applications in the future.

1.2 Literature review

1.2.1 Cy3

Cy 3 is classified as a cyanine dye. The cyanine dye was invented by Williams in 1856.[5] It is the oldest known class of synthetic dyes and has been widely used as a fluorescent probe for studying the structure and dynamics of DNA by means of fluorescence methods[4,6-8] because of their high extinction coefficient ($\sim 10^5$/mol· cm)[9] and sufficient fluorescence quantum yield ($\phi_f > 0.1$).[10] The general structure of the cyanine dye is a cationic dye typically consisting of two nitrogen atoms that are linked by a polymethine bridge with an odd number of carbons.[11] The nitrogen atom is generally a part of a heterocyclic aromatic organic compound such as indole, quinoline, benzoxazole and benzothiazole.[6,7] By varying the length of its polymethine bridge, the cyanine dye is capable of absorbing and emitting photons throughout visible and near-infrared regions.[1,2] If dividing these dyes based on the close or open chain, there are three different types. Those are streptocyanines or open chain cyanines (R_2N^+=CH[CH=CH]$_n$-NR_2), hemicyanines (Aryl=N^+=CH[CH=CH]$_n$-NR_2) and closed chain cyanines (Aryl=N^+=CH[CH=CH]$_n$-N=Aryl), where the two R's refer to the alkyl groups and n refers to a number of methine groups as shown in **Figure 1.**[12]

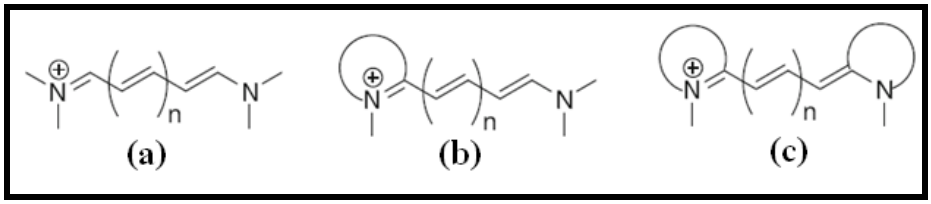

Figure 1. Generic structure of cyanine (polymethine) dyes; (a) is streptocyanine or open chain cyanine, (b) is hemicyanine and (c) is closed chain cyanine.

Cy3 is a member of closed chain cyanine dyes. In case of the close chain cyanines, they are classified by typical heterocyclic components as shown in **Figure 2.** The nitrogen atom is part of the terminal heterocyclic group and R refers to substituents, which are usually alkyl groups. For example, an indocyanine dye has indole components; a quinocyanine has quinoline groups. The common names of cyanine dyes are also in accordance to the number of methine groups in the polymethine bridge. For example, monomethine, trimethine, pentamethine and heptamethine cyanine refer to dyes having 1 (n = 0), 3 (n = 1), 5 (n = 2) and 7(n = 3) methine group in the bridge, respectively. Thus, Cy3 is also known as trimethine cyanine dye. The absorption and emission spectra of cyanine dyes are different depending on the length of the polymethine bridge and the substituent of the heterocycles.[7]

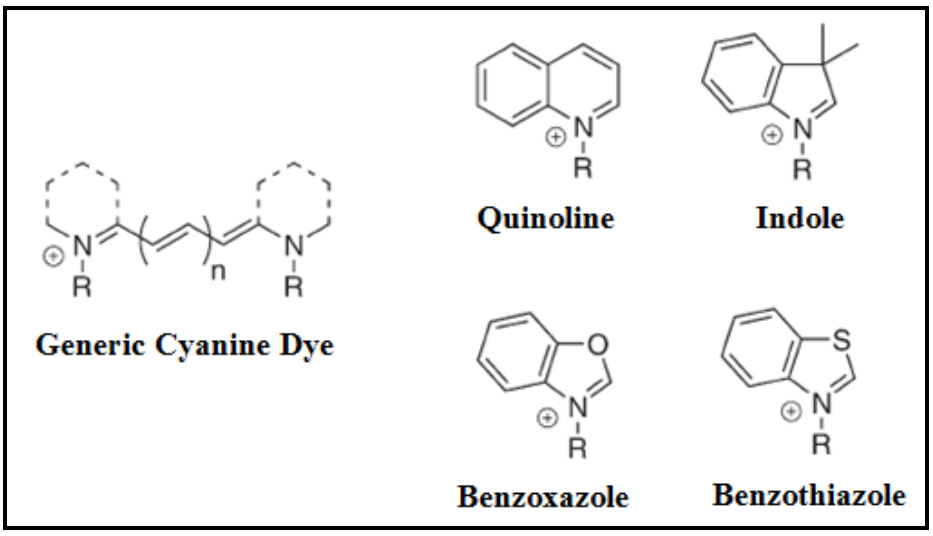

Figure 2. Generic structure of the closed chain cyanine and typical heterocyclic components.[6]

Cyanine dyes can also be classified by relating to the symmetrical or unsymmetrical structure. If the heterocycles that linked the methine bridge are the same structure and at the same position, it is called a symmetrical dye. On the other hand, if the methine bridge consists of either two different heterocycles or two identical heterocycles linked at different positions, it is called an unsymmetrical dye. Examples of the symmetrical and unsymmetrical dyes are shown in **Figure 3**.

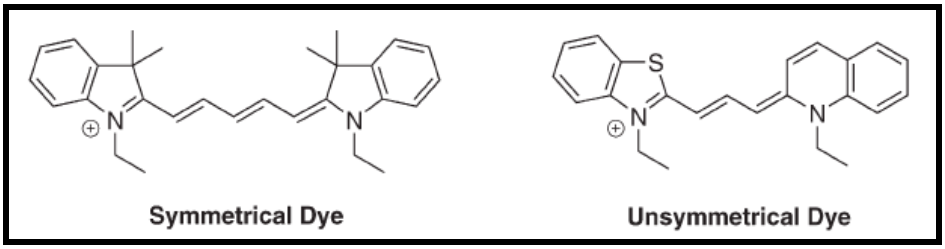

Figure 3. Examples of the symmetrical (left) and unsymmetrical (right) cyanine dyes.[7]

As shown in **Figure 4**, Cy3 is a symmetrical cyanine dye in a class of closed chain cyanine and is a planar cationic molecule in which two indole rings are linked by a trimethine bridge.[13] The bonds on the bridge are part of the conjugated system that contains π-electrons. Because of the symmetrical structure of Cy3, the electrons can have resonant delocalization within the bridge between the two indole rings on both sides.[6] Cy3 has a maximum absorption at 550 nm and a maximum emission at 570 nm in aqueous solution.[14] The absorption and fluorescence spectra are shown in **Figure 5**.

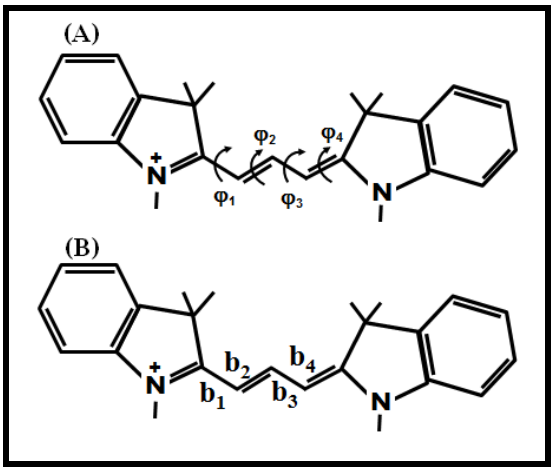

Figure 4. Free-Cy3 in *all-trans* structure in which the dihedral angles φ_1, φ_2, φ_3 and φ_4 are equal to 180^0. In *cis* structure, one of the dihedral angles has a value of 0^0. φ_i in (A) represents each dihedral angle and b_i in (B) represents each bondlength.

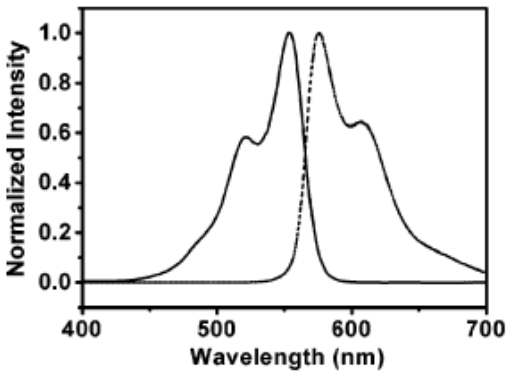

Figure 5. Normalized absorption spectrum (left) and fluorescence emission spectrum of Cy3 (right) in aqueous solution.[15]

1.2.2 Photophysics of Cy3

When a molecule absorbs a photon and an electron is raised to the higher electronic energy level, this process is called excitation or activation. It can return to the electric ground state (S_0) by both radiative and nonradiative pathways as shown in the Jablonski diagram in **Figure 6**. This process is called deactivation. The Jablonski diagram illustrates the electronic states of a molecule and the processes that happen between the absorption and emission of the energy. The symbols S_0, S_1, S_2, T_1, T_2, refer to the ground state, first excited singlet state, second excited singlet state, first excited triplet state and second excited triplet state respectively.

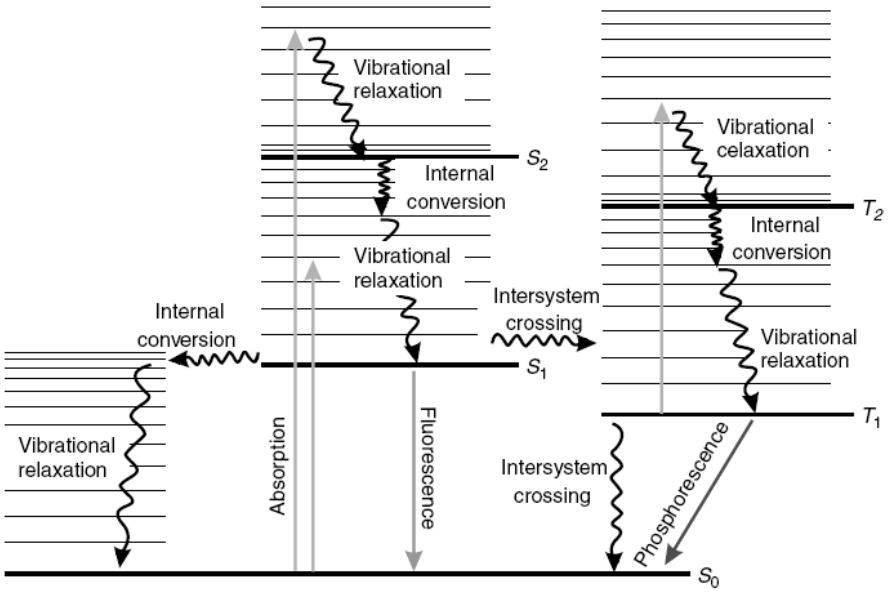

Figure 6. The Jablonski diagram.[16]

The singlet state represents the state that two electron spins are in the opposite directions (anti-parallel). On the other hand, the triplet state represents the state that two electron spins are in the same directions (parallel). [17] The spin states are shown in **Figure 7.**

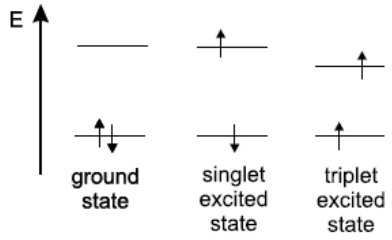

Figure 7. The electronic spin state configurations of the singlet and triplet states.

If we consider again at the Jablonski diagram, the pathways for deactivation consist of vibrational relaxation, internal conversion, intersystem crossing, phosphorescence and fluorescence. The deactivation processes can be classified into two groups; radiative and nonradiative processes. Vibrational relaxation is the nonradiative deactivation. When the molecule is promoted and resides in the higher vibrational level, the molecule quickly (between 10^{-12} – 10^{-10} seconds) loses its energy by collision with other molecules and falls to the lowest vibrational level of

this state; this process is called vibrational relaxation. In this process, when the molecule falls to the lowest vibrational level, it can later lose energy by other processes. Internal conversion is also the nonradiative deactivation without an emission of a photon. It transitions from a higher to a lower electronic state in a molecule by the same spin multiplicity, quickly within 10^{-14} – 10^{-11} seconds. Intersystem crossing is another nonradiative deactivation. It occurs between two electronic states of the different spin multiplicity. This process occurs in the time scale of 10^{-9} – 10^{-7} seconds. Phosphorescence is the radiative deactivation or a process of photon emission. The electrons transition from the lowest vibrational level of the excited triplet state to the singlet ground state. This process requires at least 10^{-4} – 10^{-2} seconds. Lastly, fluorescence is the emission of photons resulted from the transition from the singlet excited state to the singlet ground state. Such emitted photons have longer wavelength than the absorbed one. The fluorescence lifetime goes from 10^{-12} to 10^{-9} seconds.

Fluorescence method is a significant tool for investigating the structure and dynamics of matters at the molecular or atomic level because of their high sensitivity and specificity.[17] Cy3, as one of the widely used fluorescent dye has been applied in many biological system. For example, it is employed as a fluorescent label for studies of biomolecules such as nucleic acids and proteins[6,7,18-22] and is used mostly as a donor for Fluorescence Resonance Energy Transfer (FRET) measurement.[23] The local environment of Cy3 has a significant influence on its fluorescence behavior.[3,5,24] That is to say, when Cy3 is in different surroundings, it has different fluorescence properties. For example, the fluorescence quantum yield is low when Cy3 is in a solution, but increases considerably when it is bonded to a DNA. [3,4,24] The photophysics of Cy3 has been investigated extensively.[3,20,22,25] Those are concerned with the relaxation mechanisms that occur when the molecule is excited and then deactivated. There are two major pathways of deactivation from the singlet excited state to the singlet ground state ($S_1 \rightarrow S_0$) of Cy3. One is a fluorescence process and the other is a *trans-cis* isomerization (or a rotation about one of the C-C bonds of the polymethine chain).[15,26,27] These two processes compete with each other. In general, the photophysics of cyanine dye can be illustrated in

terms of the potential energy surfaces as shown in **Figure 8**.[28] On the ground state, Cy3 is stable in all-*trans* configuration.[5,8,15] After Cy3 is vertically excited to S_1, it undergoes either the fluorescence or the isomerization to return to the ground state, S_0. In the isomerization reaction, one of the bonds in the conjugated system twists, leading to the intermediate twisted state (T; $\phi = 90^0$). At this T state, Cy3 can transition rapidly to the ground state, in which it can evolve to a *cis* conformation ($\phi = 0^0$) or return back to a previous form, *trans* conformation ($\phi = 180^0$) as shown in **Figure 8**.[3,8,28-30] However in most cases, Cy3 has to surpass a barrier on S_1 in order to reach the T state. The activation energy or the energy barrier for the *trans-cis* isomerization depends strongly on Cy3's environment, especially the one that rigidifies the dye.[3,31,32] If the Cy3's backbone is rigid, it leads to the high activation energy for isomerization and thus an increased fluorescence efficiency.

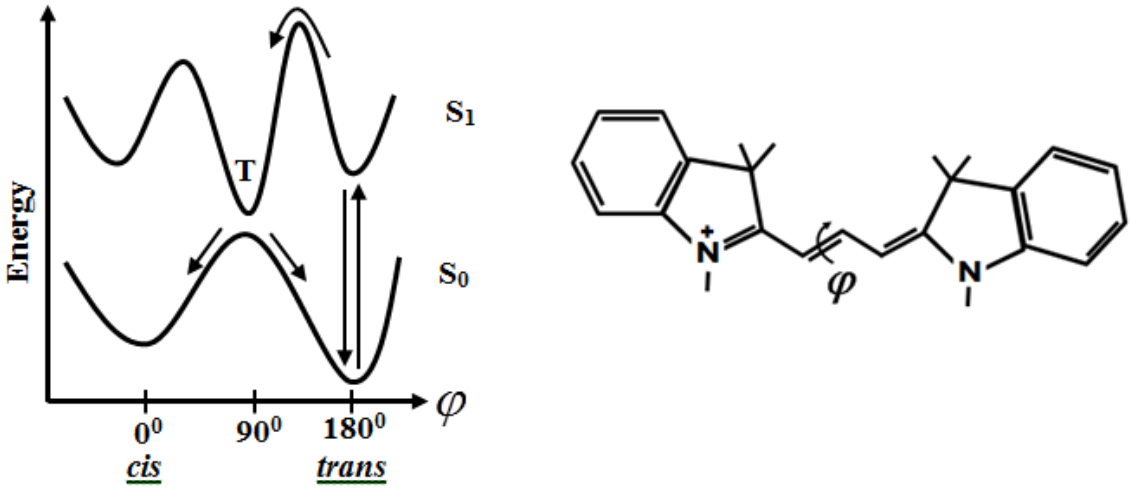

Figure 8. Schematic potential energy surface for photoisomerization of cyanine in the ground state (S_0) and the excited state (S_1). T represents the intermediate twisted state.

In their recent work, Sanborn et al.[3] have studied the fluorescence and photophysical properties of sulfoindocyanine (Cy3 with sulfonate groups) attached to the DNA, and it was shown that the dye's properties depend on its environment. The fluorescence quantum yield of Cy3 increases when bonded to DNA and shows strong relation to the energy barrier for isomerization.[3] Additionally, according to Brismar et al., the fluorescence lifetime of Cy3 is also increased when it

is conjugated to a protein.[33] Moreover, Lee et al. have shown that the non-radiative pathway from the excited state is promoted because of the lack of structural rigidity for the Cy3 molecule.[34] In addition, not only the attachment of Cy3 to DNA but also the type of the DNA base pair can affect the dye's photophysical properties, according to the study by Harvey and coworkers.[19] It was found that the fluorescence efficiency and lifetime of Cy3 are enhanced, and at the same time, the activation barrier for photoisomerization increases due to the change of attaching base pair from A-T to G-C.[19]

In spite of various experimental studies of the cyanine dyes, the isomerization and fluorescence processes can not be directly observed in a molecular level, i.e., the nuclear motion can not be seen. In order to study the dynamical phenomena of the molecules or atoms in a microenvironment, a computational simulation is a great choice for solving the interesting chemical problems of interest and investigating the physical properties of the molecules at a molecular level. This is because the molecular computer simulations enable us to determine the electronic structure and energy of the molecule, to visualize the molecular structure, and to simulate a real dynamical event, etc. The investigations of the photophysics of Cy3 and related cyanine dyes by means of computational methods have been performed by several groups. Spiriti et al. employed the DFT method to study the stacking interaction between Cy3 and the double-stranded DNA.[35] They discovered that the type of the terminal base attached to the 5′ end of a DNA duplex could affect the Cy3-DNA stacking interactions.[35] It was found that the Cy3's affinity for the T-A (with the dye attached to T) was less than for the other base pairs and it is consistent with the low energy barrier for *cis-trans* isomerization observed from the experimental results.[35] Furthermore, Sanchez-Galvez et al. had studied the ultrafast photoisomerization of three symmetric cyanine dye models with different polymethine bridge (tri-, penta- and heptamethine cyanine) by using a complete active space self consistent field (CASSCF) method.[36] They found that the activation energy for the *trans-cis* isomerization of these dyes increases with the length of the polymethine chain.[36] In Cao and coworkers' study, the time-dependent density functional theory (TDDFT) was used for the excited state calculations of the

cyanine dye and it was found that different C-C bonds in the conjugated polymethine bridge have different activation energies for isomerization, depending on its position.[31] Park had investigated the potential energy surface for the isomerization of symmetrical carbocyanines (tri- and pentamethine cyanine) by the AM1 semiempirical method and found that the length of the polymethine chain can influence the isomerization potential energy surface, i.e., the longer polymethine chain, the higher energy barrier.[37]

Up until now, there are only a handful of computational studies on the excited-state isomerization of Cy3; some of them have not considered the dynamical effects. Therefore in this work, the free energy profiles of Cy3 on the excited state are calculated to include the dynamical behavior into account. More importantly, the calculated results are then analyzed to determine the isomerization barrier that can provide a more complete explanation for the mechanisms of Cy3 deactivation when it is free and when it is attached to DNA in solvated environment. Because of the photophysics of Cy3 deactivation, i.e., fluorescence process and *trans-cis* isomerization, involves both electronic ground and excited state, the quantum mechanics (QM) method is required to describe this phenomenon. The MM method is also needed for treating the system because the surrounding of Cy3 apparently affect its photophysics.[3] Therefore, the hybrid QM/MM method[38] is used in this study. In the simulations, Cy3 is put in three different conditions. These are free Cy3 (free-Cy3); Cy3 attached to the 5′end of the single-stranded DNA (Cy3-ssDNA); and Cy3 attached to the 5′ end of the double-stranded DNA (Cy3-dsDNA). In all conditions, the free and DNA-attached Cy3 are solvated with methanol due to Cy3's low solubility and its tendency to aggregate without sulfonate group substitution in aqueous solution.[39] In addition, the effect of the stacking interaction and the binding affinity between Cy3 and the terminal base pair of DNA are investigated and discussed.

1.3 Objective

To calculate the free energies for isomerization of Cy3 in different environments by QM/MM method for more understanding of the behavior of Cy3 on the excited state.

1.4 Expected outputs from the study

1. The free energies for isomerization of Cy3 in different environments obtained from the QM/MM simulations are expected to enable a better explanation of its excited state relaxation and hence its fluorescence properties which are strongly dependent on the its surrounding.

2. The knowledge achieved from this study is expected to become a useful database of cyanine dyes for their various applications in the future.

1.5 Scope of the study

Free energy determinations of free Cy3 and Cy3 attached to single-stranded and double-stranded DNAs in methanol by QM/MM simulations.

CHAPTER 2

THEORIES

2.1 Hybrid quantum mechanics/molecular mechanics method (QM/MM)

The quantum mechanics/molecular mechanics (QM/MM) technique is used in this work to study the quantum effects of Cy3 in the excited state while including the effect of Cy3's surrounding when it is bonded and not bonded to DNA in methanol. Cy3 is treated by QM while DNA and methanol is treated by MM.

In 1976, the QM/MM approach was introduced by Warshel and Levitt.[1] They were later awarded the 2013 Nobel Prize with Kaplus for pioneering the QM/MM method. At the beginning, they applied it to study the reaction catalyzed by the enzyme, lysozyme.[1] In QM/MM method, the system is divided into the inner region that is treated with QM principles and the outer region that is treated with MM method. The total Hamiltonian of the system $\hat{H}$ is written as of

$$\hat{H}_{total} = \hat{H}_{QM} + \hat{H}_{MM} + \hat{H}_{QM/MM} \qquad (1)$$

where $\hat{H}_{QM}$ and $\hat{H}_{MM}$ are the QM and MM Hamiltonian, respectively. $\hat{H}_{QM/MM}$ is the interaction between the QM and the MM region. In this work, Cy3 is selected to be treated by QM, using a semiempirical method with the floating occupation molecular orbital configuration interaction (see 2.1.2). The environment consisting of DNA and methanol is treated by MM approach (see 2.1.1). The coupling Hamiltonian $\hat{H}_{QM/MM}$ is represented as a sum of electrostatic and van der Waals interactions:

$$\hat{H}_{QM/MM} = \hat{H}^{ES}_{QM/MM} + \hat{H}^{vdW}_{QM/MM} \qquad (2)$$

where

$$\hat{H}^{ES}_{QM/MM} = \sum_{i}^{\substack{QM\\electrons}} \sum_{m}^{\substack{MM\\atoms}} \frac{q_m}{r_{im}} + \sum_{k}^{\substack{QM\\nuclei}} \sum_{m}^{\substack{MM\\atoms}} \frac{Z_k q_m}{r_{km}}, \quad (3)$$

$$\hat{H}^{vdW}_{QM/MM} = \sum_{k}^{\substack{QM\\nuclei}} \sum_{m}^{\substack{MM\\atoms}} 4\varepsilon_{km} \left[\left(\frac{\sigma_{km}}{r_{km}} \right)^{12} - \left(\frac{\sigma_{km}}{r_{km}} \right)^{6} \right]. \quad (4)$$

The symbols *i, m* and *k* are indexes of QM electrons, MM atoms and QM nuclei, respectively. The first term of the electrostatic interactions is Coulomb interactions between the QM electrons and point charges centered on the MM atoms. The second term is Coulomb interactions between nuclear core charges of the QM atoms and point charges on the MM atoms. The r_{im} and r_{km} are distances between QM electron *i* and MM atom m; and between QM nucleus k and MM atom *m*, respectively. For the van der Waals term, σ_{km} and ε_{km} are the Lennard-Jones parameters. Specifically, σ_{km} is the distance between QM nuclei *k* and MM atom *m* at which the van der Waals interaction is zero. ε_{km} is the depth of the potential well for interaction between the two atoms (or nuclei).

2.1.1 Molecular forcefield

The potential energy surface (PES) of the MM region is calculated by a molecular forcefield. The potential energy of the system can be written in bonded and nonbonded terms. The bonded terms are composed of the energies involving the bond lengths $\left(E_{bond}\right)$, bond angles $\left(E_{angle}\right)$, and dihedral angles $\left(E_{dihedral}\right)$ among the bonded nuclei. The nonbonded terms refer to electrostatic $\left(E_{ES}\right)$ and van der Waals $\left(E_{vdW}\right)$ interactions as shown in equation (5).

$$\begin{aligned} E_{total} &= E_{bonded} + E_{nonbonded} \\ &= \left[E_{bond} + E_{angle} + E_{dihedral} \right] + \left[E_{ES} + E_{vdW} \right] \end{aligned} \quad (5)$$

$$= \left[\frac{1}{2} \sum_{bonds} k_r \left(r - r_{eq} \right)^2 + \frac{1}{2} \sum_{angles} k_\theta \left(\theta - \theta_{eq} \right)^2 + \sum_{dihedrals} \sum_{n=1}^{3} \frac{V_n}{2} \left(1 - \left(-1 \right)^n \cos\left(n\phi \right) \right) \right]$$

$$+ \sum_{i<j} \left[\frac{q_i q_j}{R_{ij}} + 4\varepsilon_{ij} \left(\frac{\sigma_{ij}^{12}}{R_{ij}^{12}} - \frac{\sigma_{ij}^{6}}{R_{ij}^{6}} \right) \right] f_{ij} \, .$$

The k_r and k_θ are force constants of bond and angle potentials, respectively. The r_{eq} and θ_{eq} are corresponding to the equilibrium lengths and angles. V_n is the amplitude of the periodic energy of the dihedral terms. In the nonbonded term $\left(E_{nonbonded} \right)$, there are two components, the Van der Waals interaction energy and the electrostatic interaction energy. The q_i and q_j are charges of atom *i* and *j* separated by a distance R_{ij}. The potential energy for van der Waals term is approximated by Lennard-Jones potential. σ_{ij} is the distance between atom i and atom j at which the van der Waals interaction is zero. ε_{ij} is the Lennard–Jones well depth and f_{ij} is a scaling factor depending on the type of non-bonded interaction between atom *i* and *j*. The f_{ij} factor is unity except for 1-4 interactions (between atoms three bonds apart) which are scale down by f_{ij} = 0.5.

For the MM part in all simulations, a methanol molecule is described by the OPLS-AA force field[2] and the DNA-bound system is described by the AMBER force fields.[3-6]

2.1.2 Semiempirical method

For the QM part, the semiempirical method is employed for the excited state calculations due to a large size of Cy3 (56 atoms). In order to maintain the multiple electronics state description for Cy3, the floating occupation molecular orbital configuration interaction (FOMO-CI) method, developed by Granucci and Toniolo,[7] is used. This method is in analogy with the complete active space self-consistent field (CASSCF),[8] a multireference approach. Similar to other multireference methods, FOMO-CI is suitable for the study of surface crossings and population transfer by employing the multiple configurations of electrons to describe the multi-

electronic state characters.[7] In this method, the orbitals in the active space are first optimized via a self-consistent field (SCF) calculation. These orbitals in the active space are allowed to have fractional occupation numbers.[7] The general Hartree-Fock form of the elements of the electronic density matrix ρ are then given as:

$$\rho_{ij} = \sum_k O_k c_{ik} c_{jk} \tag{6}$$

where c_{ik} is the k^{th} MO coefficient for the i^{th} atomic basis function. The floating occupation numbers O_k are optimized via FOMO-self consistent field calculation according to equation (7).

$$O_k = \sqrt{\frac{2}{\pi\omega^2}} \int_{-\infty}^{E_{Fermi}} \exp\left[-\frac{(E - E_k)^2}{2\omega^2} \right] dE \tag{7}$$

where ω is the width of the Gaussian function of the orbital in the active space, E_k is the energy of the orbital *k* and E_{Fermi} is the Fermi energy which is determined such that $N = \sum_k O_k$, where *N* is the total number of electrons in the system that is held constant. In the ground state, if $E_k \gg E_{Fermi}$ then $O_k \approx 0$; on the other hand if $E_k = E_{Fermi}$ then $O_k \approx 2$. The CAS-CI calculation is then performed in this active space (consisting of the optimized fractional occupied orbitals) without further orbital optimization. The FOMO-CI approach, implemented in MOPAC2000[9] package, is employed for all geometry optimizations and electronic structure calculations of the QM region, Cy3. The active space for Cy3 in this study is composed of 4 electrons in 4 orbitals. The reoptimized semiempirical parameters[10] are used for the Cy3 molecule. This parameter set is reparameterized for the conjugated systems and it was shown to have the ability to describe the multi-state characters of the photoisomerizable molecule.[10]

2.2 Full multiple spawning dynamics

To study the photoactivation of Cy3 in difference environments, it is important to take dynamical effects into account. Thus, the dynamics simulation is consequently needed. Since the dynamics of Cy3 involves nonadiabatic transition

phenomena, it is necessary to treat it with the quantum mechanical principles. The full multiple spawning method (FMS) developed by Martinez and co-workers,[11,12] is therefore used to simulate Cy3 dynamics in order to handle the nuclear quantum effects in the nonadiabatic events. This method is based on the expansion of the nuclear basis set for better describing the time-dependent wave function appearing in a multi-electronic state reaction as seen in Cy3. The total time-dependent wave function can be written as shown in equation (8) that consists of the nuclear wave function χ_I on the associated electronic state I as

$$\psi = \sum_I \chi_I(\mathbf{R};t) I(\mathbf{r};\mathbf{R}) \tag{8}$$

where the vectors $\mathbf{r}$ and $\mathbf{R}$ denote the electronic and nuclear coordinates, respectively. Here and thereafter, the bolded characters represent matrices or vectors. The nuclear wave function for each I^{th} electronic state are represented as a sum of multidimensional complex Gaussians basis functions, G_j^I.

$$\chi_I(\mathbf{R};t) = \sum_{j=1}^{N_I(t)} C_j^I(t) G_j^I(\mathbf{R};\bar{\mathbf{R}}_j^I(t),\bar{\mathbf{P}}_j^I(t),\bar{\gamma}_j^I(t),\alpha_j), \tag{9}$$

where $N_I(t)$ is a size of nuclear basis function on electronic state I at time t that changes during the course of dynamics. G_j^I is a product of 3N one-dimensional Gaussians, each represents a nuclear degree of freedom. The multi-dimensional frozen Gaussian is given as

$$G_j^I(\mathbf{R};\bar{\mathbf{R}}_j^I(t),\bar{\mathbf{P}}_j^I(t),\bar{\gamma}_j^I(t),\alpha_j) =$$
$$e^{i\bar{\gamma}_j^I(t)} \prod_\rho^{3N} \left(\frac{2\alpha_{j\rho}}{\pi}\right)^{1/4} \exp\left[-\alpha_{i\rho}\left(R_\rho - \bar{R}_{j\rho}^I(t)\right)^2 + i\bar{P}_{j\rho}^I(t)\left(R_\rho - \bar{R}_{j\rho}^I(t)\right)\right] \tag{10}$$

where ρ is the individual degrees of freedom for the nuclei. Each Gaussian basis functions is parameterized with an average position $\bar{R}_{j\rho}^I(t)$, average momentum $\bar{P}_{j\rho}^I(t)$ and Gaussian width parameter, $\alpha_{j\rho}$. The average position and momentum are solved by Hamilton's equations of motion.

$$\frac{\partial \bar{R}_{j\rho}^I}{\partial t} = \frac{\bar{P}_{j\rho}^I}{m_\rho},$$

$$\frac{\partial \bar{P}_{j\rho}^{I}}{\partial t} = \left. \frac{\partial V_{II}\left(\mathbf{R}\right)}{\partial R_{j\rho}} \right|_{\bar{R}_{j\rho}^{I}(t)} \tag{11}$$

where m_ρ and $V_{II}(\mathbf{R})$ are the mass of the ρ^{th} degree of freedom and the potential energy of the I^{th} electronic state, respectively. $\bar{\gamma}_j^I$ is the semiclassical phase, i.e., as time integrals of the Lagrangian:

$$\frac{\partial \bar{\gamma}_j^I}{\partial t} = -V_{II}\left(\bar{\mathbf{R}}_j^I(t)\right) + \sum_{\rho=1}^{3N} \frac{\left(\bar{P}_{j\rho}^I(t)\right)^2}{2m_\rho}. \tag{12}$$

The time evolution of the complex coefficient C_j^I is governed by the nuclear overlap $\left(\mathbf{S}_{II}\right)$ and Hamiltonian $\left(\mathbf{H}_{II}, \mathbf{H}_{IJ}\right)$ obtained from the nuclear Schrödinger equation.

$$\frac{\partial \mathbf{C}^I(t)}{\partial t} = -i\left(\mathbf{S}_{II}^{-1}\right)\left\{\left[\mathbf{H}_{II} - i\dot{\mathbf{S}}_{II}\right]\mathbf{C}^I + \sum_{J\neq I}\mathbf{H}_{IJ}\mathbf{C}^J\right\} \tag{13}$$

where

$$\left(S_{II}\right)_{kl} = \left\langle G_k^I \middle| G_I^I \right\rangle \tag{14}$$

and

$$\left(\dot{S}_{II}\right)_{kl} = \left\langle G_k^I \middle| \frac{\partial}{\partial t} G_l^I \right\rangle. \tag{15}$$

The Hamiltonian matrix element describes the interstate coupling between nuclear basis function on the electronics I and J as:

$$\left(\mathbf{H}_{IJ}\right)_{kl} = \left\langle G_k^I \middle| \hat{\mathbf{H}} \middle| G_l^J \right\rangle \tag{16}$$

FMS has been implemented in MOLPRO[13] and MOPAC[9] program suites. More detailed discussion can be found in many reviews.[11,12]

2.3 Umbrella sampling

The time scale for the photophysical phenomena of Cy3, starting from the excited state and eventually relaxing back to the ground state is nanoseconds.[14,15] It is thus not practical to directly simulate such event. In order to solve this problem, the umbrella sampling, developed by Valleau and Torrie,[16] is used to determine the free energy and hence the energy barrier. The height of the barrier is an indicator of how difficult for Cy3 to isomerize. The umbrella sampling

technique with the weighted histogram analysis method (WHAM)[17] is used for the calculations of the free energy along the reaction coordinate of interest. This technique is designed to sample the energy landscape especially in the high-energy regions by adding a biasing (umbrella) potential to ensure that the sampling cover the whole range of the reaction coordinate.[16] Such technique enables the access to the rare event (high energy), which might take much longer time to reach with direct dynamics simulation. The two important equations of the umbrella sampling method are shown in equation (17) and (18).

$$V(R,\xi_r) = V_0 + U(\xi_r) \tag{17}$$

$$= V_0(R) + k(\xi_r - \xi_0)^2 . \tag{18}$$

Here, V_0 is the normal potential, U is the umbrella potential, *R* is the nuclear coordinate, ξ_r and ξ_0 refer to the sampling reaction coordinate and fixed reaction coordinate of interest, respectively, and k is the force constant. The reaction coordinate of interest is divided into N_w windows, as shown in **Figure 9**. Each window has its different constraint reaction coordinate, $\xi_{0,i}$. In this work, the reaction coordinates of interest are the dihedral angles φ_2 and φ_3 of the conjugated bridge shown in **Figure 4** in Chapter 1. The two dihedral angles are centered at the bonds that can rotate in the excited-state isomerization process of Cy3.[15,18-20] The umbrella sampling is performed for one dihedral angle at a time. First, φ_2 is decreased from 180^0 (*trans* configuration) to 70^0 with 10^0 increments for each window. The same approach is then applied for φ_3.

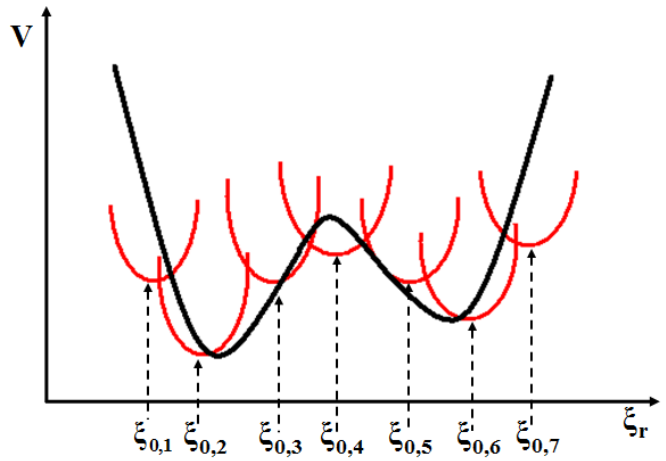

Figure 9. Principle of umbrella sampling (red = umbrella potential)

After finishing the dynamics for the umbrella sampling in all windows. The free energies calculated from the probability distributions (these are the biased probability distributions) of each window are combined together (**Figure 10**, upper panel) and then adjusted with the WHAM method[17] to remove the effect of biasing umbrella potential (**Figure 10,** lower panel) to get the unbiased probability distribution $P(\xi_r)$ and the free energy shift F_i for the i^{th} window. The non-biased free energy can be estimated using two key equations.[17]

$$P(\xi_r) = \frac{\sum_{i=1}^{N_w} n_i(\xi_r)}{\sum_{i=1}^{N_w} M_i \left[F_i - U_{bias,i}(\xi_r) \right] / k_B T}, \tag{19}$$

$$F_i = -k_B T \ln\left(\sum_{\xi_{bins}} P(\xi_r) \exp\left[-U_{bias,i}(\xi_r) / k_B T \right] \right). \tag{20}$$

The $n_i(\xi_r)$ refers to the number of count in histogram bin associated with ξ_r, M_i is the total number of data taken from the i^{th} window and $U_{bias,i}(\xi_r)$ is the biased umbrella potential.[17] The sum in equation (20) is over ξ_{bins}, which include every bin associated with ξ_r. The two WHAM equations above have to be solved by iteration to self-consistency because neither F_i nor $P(\xi_r)$ are known beforehand. After

removing the umbrella potential, the relative free energy is obtained from equation (21).

$$\Delta F(\xi_r) \propto -k_B T \log\left[P(\xi_r)\right]$$
$$\approx -\frac{2}{3N}\left\langle E_{kinetic}\right\rangle \log\left[P(\xi_r)\right]. \quad (21)$$

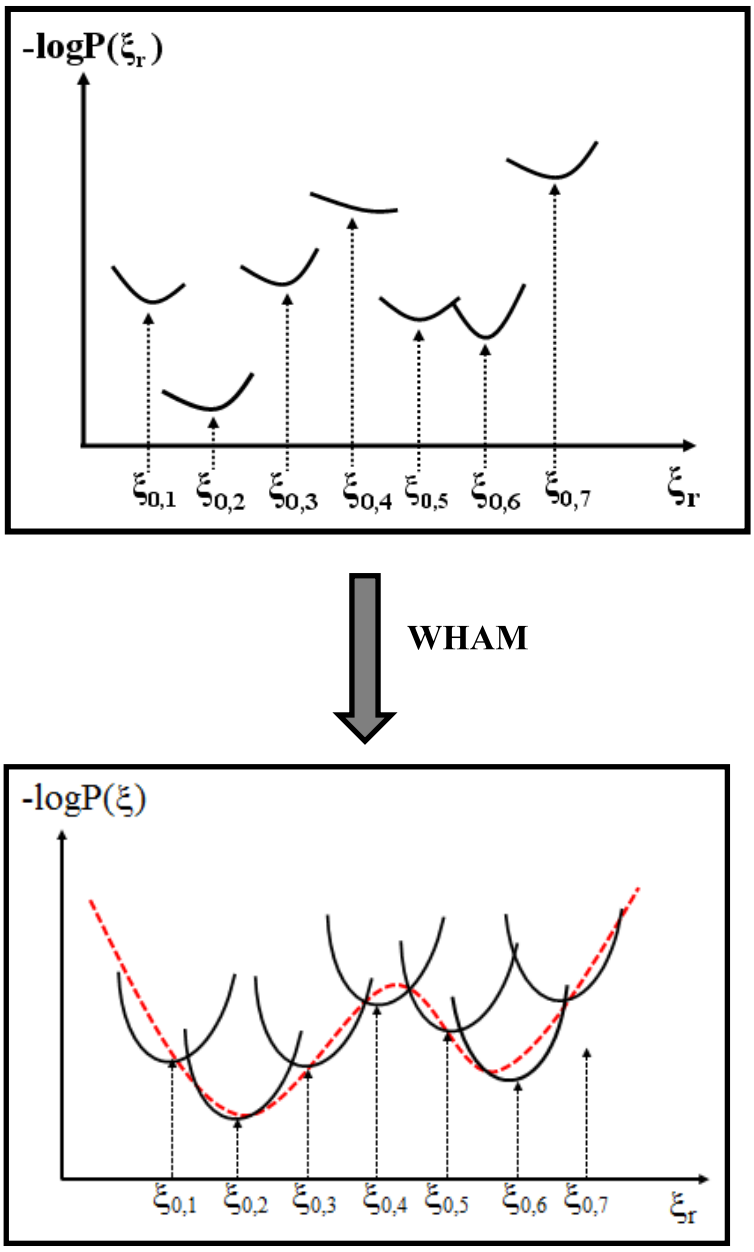

Figure 10. Debiasing of the probability distribution. First the biased free energies from N_w windows are combined together. Then the free energy of each window is moved up or down by WHAM in the process of getting rid of the umbrella potential.

(1) Warshel, A.; Levitt, M.: Theoretical Studies of Enzymic Reactions : Dielectric, Electrostatic and Steric Stabilization of the Carbonium Ion in the Reaction of Lysozyme. *J. Mol. Biol.* **1976**, *103*, 227-249.

(2) Jorgensen, W. L.; Maxwell, D. S.; Tirado-Rives, J.: Development and Testing of the OPLS All-Atom Force Field on Conformational Energetics and Properties of Organic Liquids. *J. Am. Chem. Soc.* **1996**, *118*, 11225-11236.

(3) Case, D. A.; Pearlman, D. A.; Caldwell, J. W.; III, T. E. C.; Wang, J.; Ross, W. S.; Simmerling, C. L.; Darden, T. A.; Merz, K. M.; Stanton, R. V.; Cheng, A. L.; Vincent, J. J.; Crowley, M.; Tsui, V.; Gohlke, H.; Radmer, R. J.; Duan, Y.; Pitera, J.; , J.; Massova, I.; Seibel, G. L.; Singh, U. C.; Weiner, P. K.; Kollman, P. A.: *AMBER 7*: University of California: San Francisco, CA, USA, 2002.

(4) Cornell, W.; Cieplak, P.; Bayly, C.; Gould, I.; Merz, J. K.; Ferguson, D.; Spellmeyer, D.; Fox, T.; Caldwell, J.; Kollman, P.: A Second Generation Force Field for the Simulation of Proteins, Nucleic Acids, and Organic Molecules. *J. Am. Chem. Soc.* **1995**, *117*, 5179-5197.

(5) Kollman, P. A.; Weiner, P. K.: AMBER: Assisted model building with energy refinement. A general program for modeling molecules and their interactions. *J. Comput. Chem.* **1981**, *2*, 287-303.

(6) Weiner, S. J.; Kollman, P. A.; Case, D. A.; Singh, U. C.; Ghioand, C.; Alagona, G.; Jr., S. P.; Weiner, P.: A New Force Field for Molecular Mechanical Simulation of Nucleic Acids and Proteins. *J. Am. Chem. Soc.* **1984**, *106*, 765-784.

(7) Granucci, G.; Toniolo., A.: Molecular gradients for semiempirical CI wavefunctions with floating occupation molecular orbitals. *Chem. Phys. Lett.* **2000**, *32*, 79-85.

(8) Roos, B. O.: The Complete Active Space Self-Consistent Field Method and its Applications in Electronic Structure Calculations. *Adv. Chem. Phys.* **1987**, *69*, 399.

(9) Stewart, J. J. P.: *MOPAC 2000*; Fujitsu Limited: Tokyo, Japan, 1999.

(10) Owens, J. M.: Theoretical Studies of the Solvation, Dynamics, and Photochemistry of Ethylene, Retinal Protonated Schiff Base, Oligocellulose, and GD(III) Clusters. University of Illinois at Urbana-Champaign, Urbana, 2004.

(11) Ben-num, N.; Martínez, T. J.: Ab initio quantum molecular dynamics. *Adv. Chem. Phys.* **2002**, *121*, 439.

(12) Ben-Nun, M.; Quenneville, J.; Martínez, T. J.: Ab Initio Multiple Spawning: Photochemistry from First Principles Quantum Molecular Dynamics. *J. Phys. Chem. A* **2000**, *104A*, 5161.

(13) Werner, H. J.; Knowles, P. J.; Lindh, R.; Schuetz, M.; Celani, P.; Korona, T.; Manby, F. R.; Rauhut, G.; Amos, R. D.; Bernhardsson, A.; Berning, A.; Cooper, D. L.; Deegan, M. J. O.; Dobbyn, A. J.; Eckert, F.; Hampel, C.; Hetzer, G.; Lloyd, A. W.; McNicholas, S. J.; Meyer, W.; Mura, M. E.; Nicklass, A.; Palmieri, P.; Pitzer, R.; Schumann, U.; Stoll, H.; Stone, A. J.; Tarroni, R.; Thorsteinsson, T.: MOLPRO, 2006.1. **2006**.

(14) Valeur, B.: *Molecular Fluorescence: Principles and Applications*; Wiley-VCH., 2002.

(15) Sanborn, M. E.; Connolly, B. K.; Gurunathan, K.; Levitus, M.: Fluorescence Properties and Photophysics of the Sulfoindocyanine Cy3 Linked Covalently to DNA. *J. Phys. Chem.* **2007**, *111*, 11064-11074.

(16) Torrie, G. M.; Valleau, J. P.: Non-Physical Sampling Distributions in Monte-Carlo Free-Energy Estimation - Umbrella Sampling. *J. Comput. Phys.* **1977**, *23*, 187-199.

(17) Kumar, S.; Djamal, B.; Robert, S.; P.Kollmana; Rosenbergl, J.: The Weighted Histogram Analysis Method for Free-Energy Calculations on Biomolecules. I. The Method. *J. Comput. Chem.* **1992**, *13*, 1011-1021.

(18) Cao, J.; Wu, T.; Hu, C.; Liu, T.; Sun, W.; Fan, J.; Peng, X.: The nature of the different environmental sensitivity of symmetrical and unsymmetrical cyanine dyes: an experimental and theoretical study. *Phys. Chem. Chem. Phys.* **2012**, *14*, 13702-13708.

(19) F., W. S.; Zhou, T.; Huang, Y. C.; Ye, S. Y.: DFT Investigation on the Trans-cis Photoisomerization of Pentamethine Cyanine Dye Model Molecule. *Chinese J. Struct. Chem.* **2011**, *30*, 401-411.

(20) Rodríguez, J.; Scherlis, D.; Estrin, D.; Aramendía, P. F.; Negri, R. M.: AM1 Study of the Ground and Excited State Potential Energy Surfaces of Symmetric Carbocyanines. *J. Phys. Chem. A.* **1997**, *101*, 6998-7006.

CHAPTER 3

METHODOLOGY

3.1 Geometry optimization of Cy3 in isolation

The semiempirical FOMO-CI method is used to optimized Cy3 via the modified version of MOPAC2000 program[1] in order to obtain the stable structure whose energy is minimal. The optimizations are performed in both electronic ground (S_0) and excites state (S_1).

3.2 Rigid torsion cut of free-Cy3 in isolation

A major reaction coordinate for non-radiative relaxation of Cy3 is the torsional motion of its conjugated backbone, which could be the rotation of either dihedral angle φ_2 or φ_3 shown in **Figure 4**. From the experiments, these two dihedral angles can undergo the excited-state *trans-cis* isomerization of Cy3.[2-5] The rigid torsion cut which is the potential energy as a function of dihedral angles is then calculated in order to investigate the relation between the potential energy and the change in dihedral angle. The rigid torsion cut is obtained by changing only the dihedral angle φ_2 while constraining all other degrees of freedom from the optimized structure and then calculating the potential energy of the ground (S_0) and first excited (S_1) states. For the calculations from S_0-optimized geometry, the dihedral angle φ_2 was fixed at 180^0, 170^0, ..., 70^0 and then at each value of φ_2, the potential energy of S_0 and S_1 states are calculated using the reoptimized semiempirical method mentioned in Chapter 2. For the calculations on S_1, the initial geometry is the S_1-optimized structure and the process is the same as for the calculation on S_0. The potential energies of S_0 and S_1 are then plotted as a function of dihedral angle

φ_2 in both cases of the ground and the excited state optimized geometries. The rigid torsion cut is also performed in the case of the dihedral angle φ_3.

3.3 Optimization of free Cy3 in methanol

This step is for finding the stable structure of Cy3 in methanol by generating a box of methanol (CH_2OH) and determining the suitable size of the box along x-, y- and z-axis. The suitable size means that Cy3 should be surrounded by 2-3 shells of methanol molecules composing such solvation box. The stable solvated system is obtained from optimization by QM/MM method. The semiempirical method is used to treat Cy3 (QM part) and the MM forcefield is used to treat the methanol molecules. The MM force field for methanol is OPLS-AA.[6] The best result is chosen by checking if Cy3 is enclosed by 2-3 layers of methanol molecules in all direction. This is done by using a visualization program called Visual Molecular Dynamics (VMD).[7] More importantly, the energy of the chosen system should be minimal.

3.4 Calculation of the free energy of free Cy3 using 1-dimentional umbrella sampling

The umbrella sampling is performed for one dihedral angle at a time. First, φ_2 of Cy3 is decreased from 180^0 (*trans* configuration) to 70^0 with 10^0 increments for each window. Then the dynamics simulation in an individual window is performed on the excited state for 2 ps by umbrella sampling[8] implemented in the FMS program suite.[9,10] The conservation of the total energy of the system is examined. After finishing the dynamics for the umbrella sampling in all windows, the probability distributions of each window is combined together and debiased for the actual free energy with the WHAM[11] method. Then the graph of the free energy as a function of dihedral angle φ_2 in the first excited state is plotted. The free energy calculation is also performed in the case of the dihedral angle φ_3.

3.5 Geometry optimization of Cy3 attached to DNA in methanol

This step is for finding the stable structure of Cy3 attached to a single-strand (Cy3-ssDNA) and double-strand DNA (Cy3-dsDNA) (**Figure 11**) in methanol by generating a box of methanol (CH_2OH) and determining the suitable size of the box along x-, y- and z-axis. The ssDNA is five base long and the sequence is T-T-C-T-T (T is the thymine base and C is the cytosine base). For the dsDNA, the same sequence used in ssDNA is used as a primary strand, and the complimentary strand has the same length. The suitable size of the solvation box means that the Cy3-DNA system should be surrounded by 2-3 shells of methanol molecules composing such solvation box. The stable solvated system is obtained from the optimization by QM/MM method. The semiempirical method is used to treat Cy3 (QM part) and MM is used to treat the DNA and methanol molecules. The MM force field for DNA and methanol is AMBER.[12-15] The best result is chosen by checking if the Cy3-DNA system is enclosed by 2-3 layers of methanol molecules in all direction. This is done by using VMD.[7] The energy of the chosen system is also determined if it is minimal.

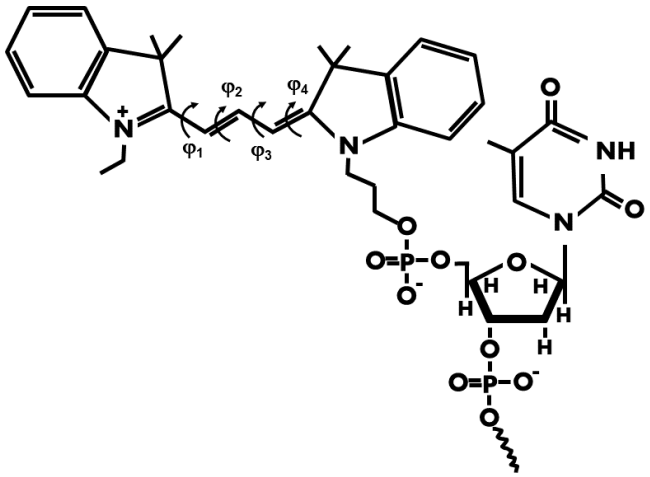

Figure 11. Structure of Cy3 attached DNA. The wavy line in the structure represents the nucleotide bonding to DNA. The dihedral angle φ_1, φ_2, φ_3 and φ_4 are defined to describe each torsional motion of Cy3.

3.6 Calculation of the free energy of Cy3-ssDNA and Cy3-dsDNA in MeOH using 1-dimentional umbrella sampling

For both cases of Cy3-ssDNA and Cy3-dsDNA, the umbrella sampling is performed for one dihedral angle at a time. Similar to 3.4, φ_2 of Cy3 is decreased from 180^0 (*trans* configuration) to 70^0 with 10^0 increments for each window. The FMS[9,10] dynamics simulation on excited state are then performed for 2 ps by umbrella sampling[8] on each window. The total energy of the system must be checked for conservation condition. After the dynamics for the umbrella sampling in all windows are completed, the probability distributions of each window are combined and debiased with WHAM[11] for the unbiased free energy. The free energy as a function of dihedral angle φ_2 in the first excited state is then generated. The free energy calculation is also performed in the case of the dihedral angle φ_3 of Cy3 attached to ssDNA and dsDNA.

(1) Stewart, J. J. P.: *MOPAC 2000*; Fujitsu Limited: Tokyo, Japan, 1999.

(2) Cao, J.; Wu, T.; Hu, C.; Liu, T.; Sun, W.; Fan, J.; Peng, X.: The nature of the different environmental sensitivity of symmetrical and unsymmetrical cyanine dyes: an experimental and theoretical study. *Phys. Chem. Chem. Phys.* **2012**, *14*, 13702-13708.

(3) F., W. S.; Zhou, T.; Huang, Y. C.; Ye, S. Y.: DFT Investigation on the Trans-cis Photoisomerization of Pentamethine Cyanine Dye Model Molecule. *Chinese J. Struct. Chem.* **2011**, *30*, 401-411.

(4) Sanborn, M. E.; Connolly, B. K.; Gurunathan, K.; Levitus, M.: Fluorescence Properties and Photophysics of the Sulfoindocyanine Cy3 Linked Covalently to DNA. *J. Phys. Chem.* **2007**, *111*, 11064-11074.

(5) Rodríguez, J.; Scherlis, D.; Estrin, D.; Aramendía, P. F.; Negri, R. M.: AM1 Study of the Ground and Excited State Potential Energy Surfaces of Symmetric Carbocyanines. *J. Phys. Chem. A.* **1997**, *101*, 6998-7006.

(6) Jorgensen, W. L.; Maxwell, D. S.; Tirado-Rives, J.: Development and Testing of the OPLS All-Atom Force Field on Conformational Energetics and Properties of Organic Liquids. *J. Am. Chem. Soc.* **1996**, *118*, 11225-11236.

(7) Humphrey, W.; Dalke, A.; Schulten, K.: VMD: Visual Molecular Dynamics. *J. Mol. Graph.* **1996**, *14*, 33-38.

(8) Torrie, G. M.; Valleau, J. P.: Non-Physical Sampling Distributions in Monte-Carlo Free-Energy Estimation - Umbrella Sampling. *J. Comput. Phys.* **1977**, *23*, 187-199.

(9) Ben-num, N.; Martínez, T. J.: Ab initio quantum molecular dynamics. *Adv. Chem. Phys.* **2002**, *121*, 439.

(10) Ben-Nun, M.; Quenneville, J.; Martínez, T. J.: Ab Initio Multiple Spawning: Photochemistry from First Principles Quantum Molecular Dynamics. *J. Phys. Chem. A* **2000**, *104A*, 5161.

(11) Kumar, S.; Djamal, B.; Robert, S.; P.Kollmana; Rosenbergl, J.: The Weighted Histogram Analysis Method for Free-Energy Calculations on Biomolecules. I. The Method. *J. Comput. Chem.* **1992**, *13*, 1011-1021.

(12) Case, D. A.; Pearlman, D. A.; Caldwell, J. W.; III, T. E. C.; Wang, J.; Ross, W. S.; Simmerling, C. L.; Darden, T. A.; Merz, K. M.; Stanton, R. V.; Cheng, A. L.; Vincent, J. J.; Crowley, M.; Tsui, V.; Gohlke, H.; Radmer, R. J.; Duan, Y.; Pitera, J.; , J.; Massova, I.; Seibel, G. L.; Singh, U. C.; Weiner, P. K.; Kollman, P. A.: *AMBER 7*: University of California: San Francisco, CA, USA, 2002.

(13) Cornell, W.; Cieplak, P.; Bayly, C.; Gould, I.; Merz, J. K.; Ferguson, D.; Spellmeyer, D.; Fox, T.; Caldwell, J.; Kollman, P.: A Second Generation Force Field for the Simulation of Proteins, Nucleic Acids, and Organic Molecules. *J. Am. Chem. Soc.* **1995**, *117*, 5179-5197.

(14) Kollman, P. A.; Weiner, P. K.: AMBER: Assisted model building with energy refinement. A general program for modeling molecules and their interactions. *J. Comput. Chem.* **1981**, *2*, 287-303.

(15) Weiner, S. J.; Kollman, P. A.; Case, D. A.; Singh, U. C.; Ghioand, C.; Alagona, G.; Jr., S. P.; Weiner, P.: A New Force Field for Molecular Mechanical Simulation of Nucleic Acids and Proteins. *J. Am. Chem. Soc.* **1984**, *106*, 765-784.

CHAPTER 4

RESULTS AND DISCUSSION

4.1 The optimized geometry of Cy3 in gas phase

The optimized structure of Cy3 is shown in **Figure 12**. From the optimization in the ground state and the excited state, Cy3 is in all-*trans* configurations, in which φ_1, φ_2, φ_3 and φ_4 (see **Figure 4**.) equal to 180^0 and the conjugated carbon bridge are in planar with both of the indole rings.

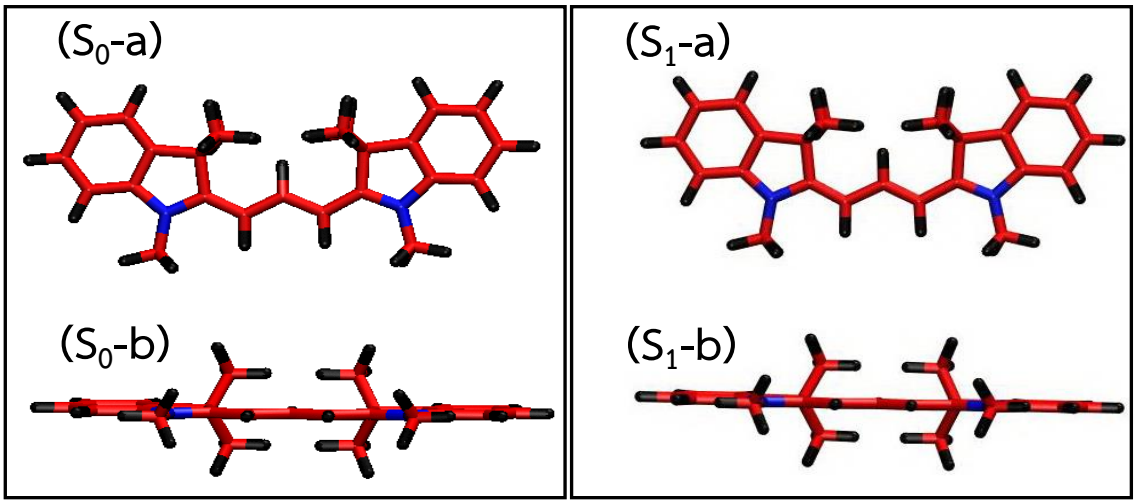

Figure 12. The optimized structure of Cy3 on the ground state, shown in top view (S_0-a) and side view (S_0-b) and on the excited state, shown in top view (S_1-a) and side view (S_1-b). The red color represent C atoms, blue is for N atoms and black is for H atoms.

4.2 The rigid torsion cut of free-Cy3 in isolation

For the potential energy calculations from the rigid torsion cut, the relative energies of Cy3 on S_0 and S_1 as the functions of φ_2 and φ_3 are shown in **Figure 13**. In all rigid torsion cuts, the potential energy profile of S_0 is peaked at 90^0 with the height varies from 36.6 to 48.7 kcal/mol, indicating difficulty of isomerization on the ground state.

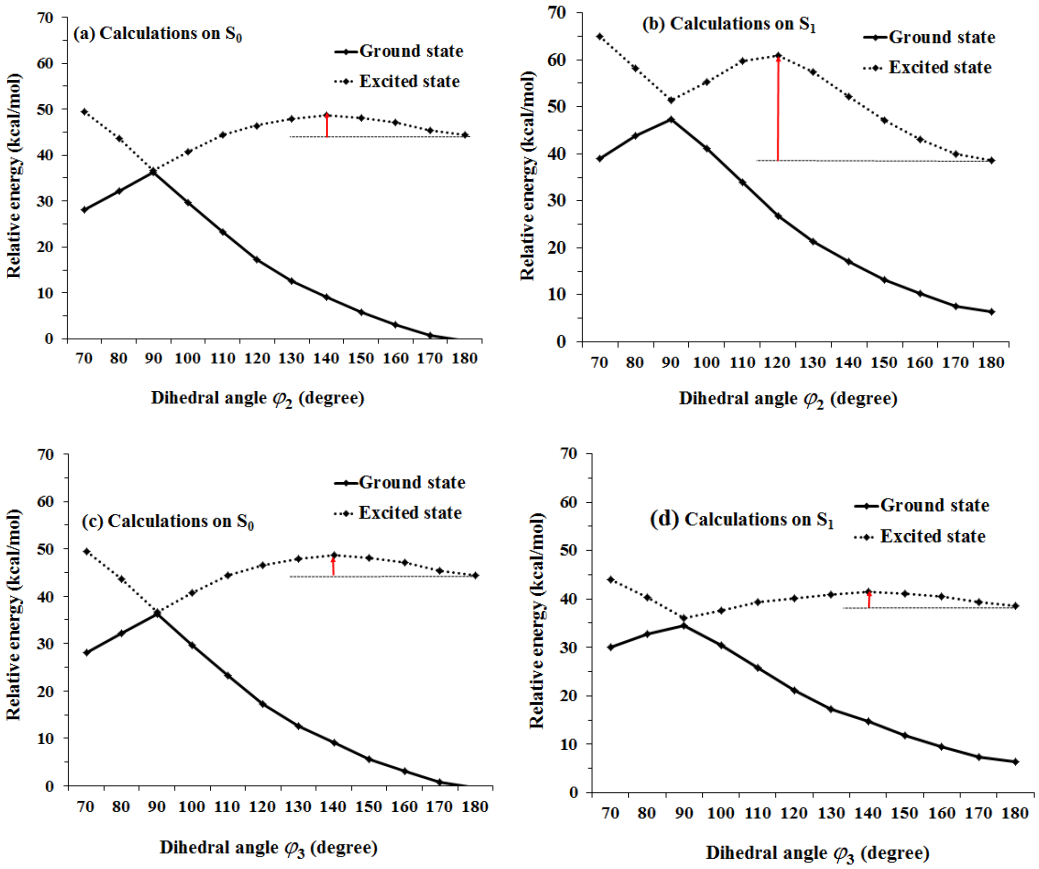

Figure 13. The rigid torsion cut of Cy3 for the rotation of φ_2 calculated on S_0-optimized geometry (a) and S_1-optimized geometry (b). The rigid torsion cut for the rotation of φ_3 calculated on S_0-optimized geometry (c) and S_1-optimized geometry (d). The relative potential energy surfaces of S_0 are represented by solid line and the one of S_1 are represented by dotted line. The vertical arrow in each panel represents the energy barrier for the S_1 isomerization measured from the all-*trans* ($\varphi = 180^0$) geometry.

Table 1. The energy barrier for *trans-cis* isomerization obtained from the rigid torsion cuts calculated on S_0 and S_1 optimized structures.

Dihedral angle	Energies barrier for *trans-cis* isomerization on S_1 state (kcal/mol)	
	Optimized on S_0 state	Optimized on S_1 state
φ_2	4.3	22.3
φ_3	4.2	3.0

As shown in **Table 1**, the energy barriers on S_1 for φ_2 and φ_3 are equal at approximately 4 kcal/mol when calculated on S_0-optimized geometry. This is not surprising because both twisting C-C bonds in the polymethine chain have almost identical bond length, as shown in **Figure 14.** Moreover, the bond length alternation of the conjugated trimethine bridge is very small and all four C-C bonds have an intermediate characteristic between the single and double bond. Therefore it is not very difficult to rotate around these bonds and leads to a very small rotational barrier. The barrier peak is located at about 140^0 dihedral angle of both φ_2 and φ_3.

In the case of the calculation on S_1-optimized geometry, the energy barriers on S_1 for φ_2 and φ_3 are approximately 22.3 and 3.0 kcal/mol, respectively. The barrier peak is located at about 120^0 dihedral angle for φ_2. For φ_3, the much smaller barrier peak is located at about 140^0 dihedral angle. For this optimized geometry on S_1, b_2 (the center bond of φ_2) shows a double-bond characteristic, while b_3 (the center bond of φ_3) shows a single bond one (see **Figure 14**). The twisting of φ_3 is therefore easier than that of φ_2 and hence showing the lower energy barrier for isomerization at φ_3 than at φ_2.

As shown in **Figure 13**, the maximum on the ground state from S_0 and S_1-optimized structure of both angles coincide with the minimum on the excited state at $\varphi = 90^0$. This energy profile is consistent with Cao and coworker's calculations using the time-dependent density functional theory (TDDFT) for

potential energy surfaces of the Cy3.[1] It was found that at $\varphi = 90^0$, a minimum exists in the S_1 potential energy surface .[1]

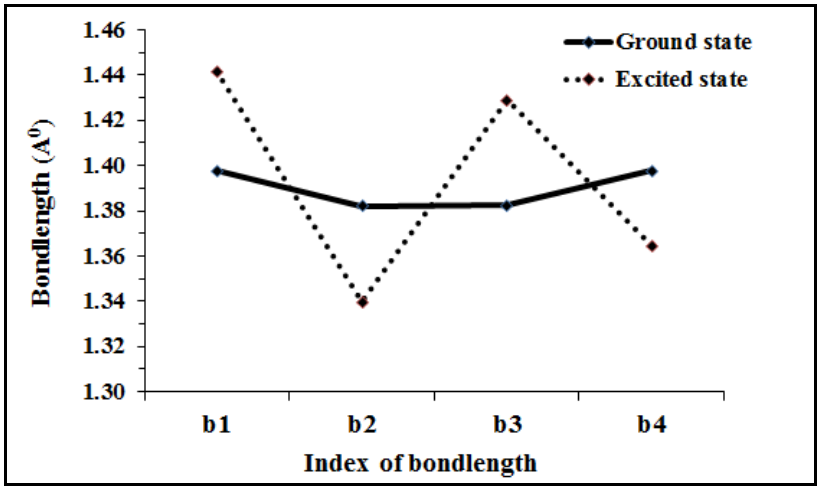

Figure 14. The bondlength of free-Cy3 molecule from the optimizations in the ground state (solid line) and the excited state (dotted line).

These results verify that due to the much lower barrier, Cy3 is more likely to undergo the *trans-cis* isomerization process in the first excited state rather than in the ground state by twisting one of the bonds on the polymethine bridge toward the S_1 energy minimum at 90^0. However, it has to surpass the barrier at around 120^0 of the dihedral angle. At 90^0-twisted geometry, the energy gap approaches zero where Cy3 can easily return to the ground state via the nonadiabatic transition and then complete the other half of the isomerization process. Therefore, the height of energy barrier does influence the *trans-cis* isomerization efficiency as well as the non-radiative relaxation. However, one of the activation energies for free-Cy3 from rigid torsion cut is very low or considered as nearly barrierless. As a result, Cy3 is easily twisted and leads to low efficiency for fluorescence process. Although the rigid torsion cuts can be used as a guideline for describing the *trans-cis* isomerization of Cy3, its shortcoming is the complete constraint on the molecule. Therefore, the further investigation is necessary to take the dynamical effect into account as will be discussed in the free energy calculations.

4.3 The optimized geometry of Cy3 in methanol

The various sizes of the methanol box that contains Cy3 as well as their energies from the optimizations are shown in **Table 2**.

Table 2. The size of the box that contains Cy3 and methanol and the total energy of the system.

Time	Size of box (Bohr)			Energy (eV)
	X	Y	Z	
1	53	37	36	-3837.29
2	54	37	36	-3835.91
3	53	38	36	-3837.02
4	53	36	36	-3836.88
5	53	37	37	-3836.74
6	53	37	35	-3836.69

The optimized structure of Cy3 in methanol is obtained from the 4^{th} condition as shown in **Figure 15**. This structure has a suitable size of the solvation box, in which Cy3 is surrounded by 2-3 shells of methanol molecules and the energy of the chosen system is comparable to other conditions. The lengths along the x-, y- and z-axis are 53, 36 and 36 Bohr, respectively.

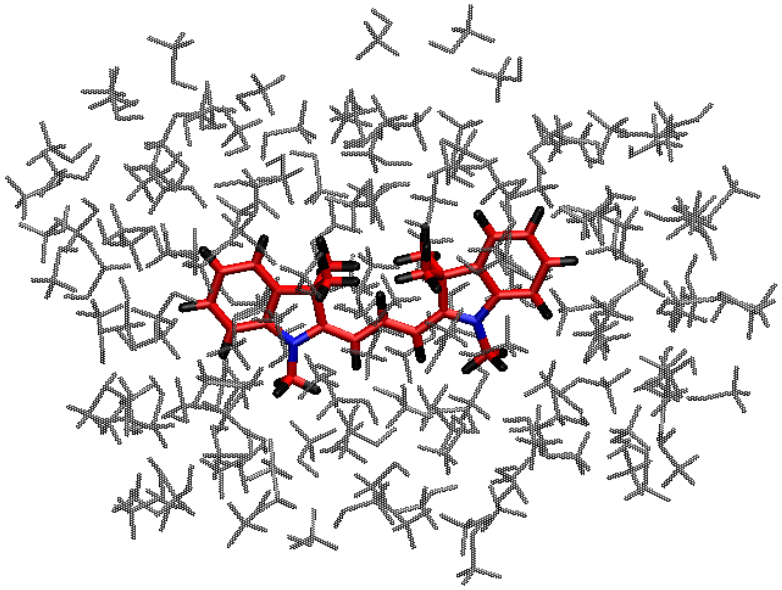

Figure 15. The optimized structure of Cy3 in methanol. The red color represents C atoms, blue is for N atoms and black is for H atoms in Cy3. The methanol molecules are displayed in gray color.

4.4 The free energy of free Cy3 using 1-dimentional umbrella sampling

This result will discuss in section **4.7** (compare free Cy3 with Cy3-DNA system)

4.5 The optimized geometry of Cy3 attached to DNA in methanol

In all simulations in the case of DNA bound, Cy3 is stacked on a DNA base as it is one of the local minima. In this stacking configuration, one indole ring of Cy3 is stacked on top of the first base of the DNA strand linked to Cy3 as shown in **Figure 16**. The initial base on the 5' end of the DNA strand binding to Cy3 in all cases is thymine (T) and Cy3 is linked to DNA via a three-carbon linker. Cy3 is in all-*trans* configurations and has planar structure.

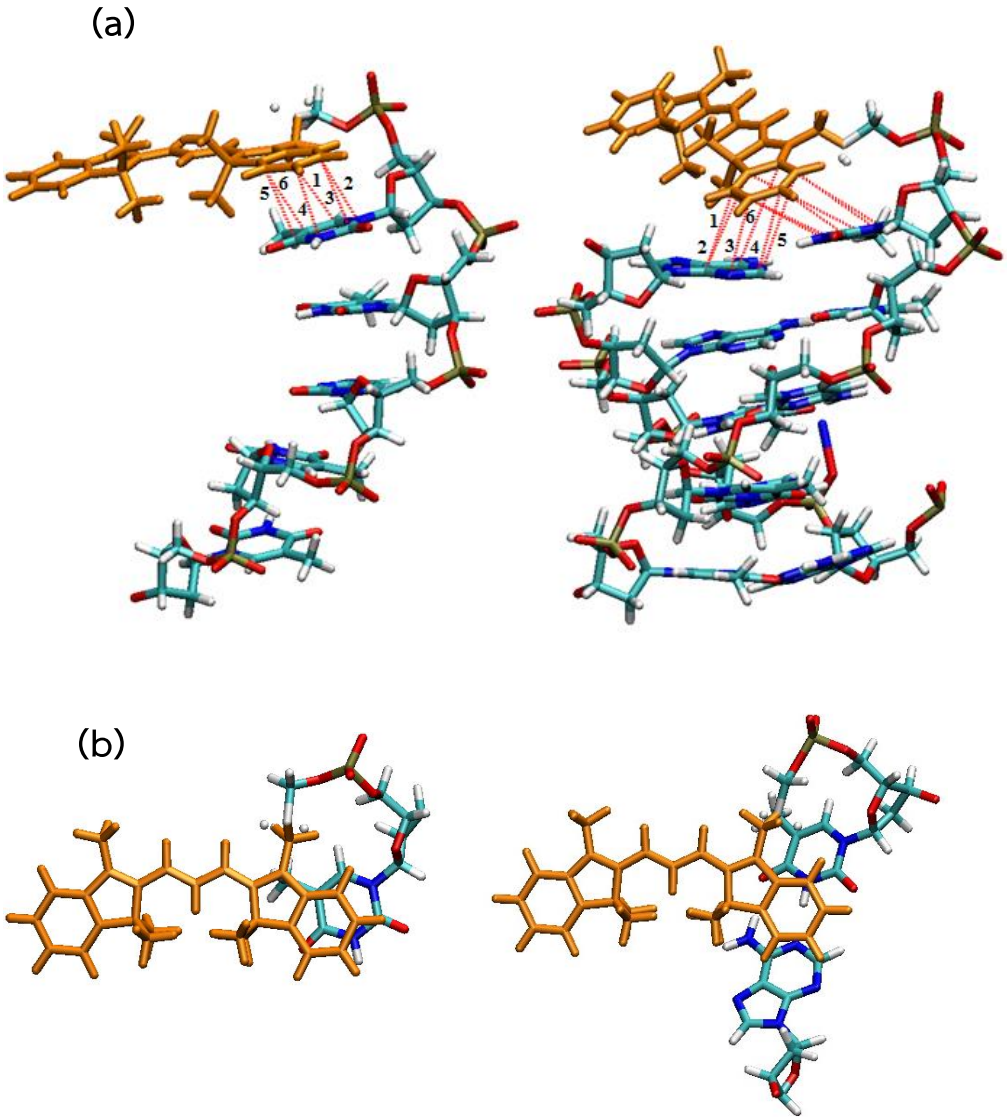

Figure 16. The configurations showing the stacking of Cy3-ssDNA and Cy3-dsDNA from (a) side view and (b) top view. The red dotted lines are distance of stacking between the ring of terminal indole of Cy3 and the first base of DNA strand. Indexs 1, 2, 3, 4, 5 and 6 represent the stacking distances between each C-atom on Cy3 and C- or N-atoms on the DNA bases. Cy3 is shown in orange. For the DNA strands, C, N, O, P and H atoms are in cyan, blue, red, tan and white colors, respectively.

The various sizes of the methanol box that contains Cy3 as well as their corresponding energies from the optimizations are shown in **Table 3**.

Table 3. The size of the box that contains Cy3-DNA and methanol and the total energy of the system.

Type of DNA	The distance of the methanol box extending from the Cy3-DNA	Energy (eV)
Cy3-ssDNA	3.9	-3933.25
Cy3-ssDNA	4.2	-3937.06
Cy3-dsDNA	4.2	Error
Cy3-dsDNA	4.5	-4014.57

The optimized structures of Cy3-ssDNA and Cy3-dsDNA in methanol are shown in **Figure 17**. This structure has the suitable solvation box as the Cy3-DNA system is surrounded by 2-3 shells of methanol molecules and the energy of the chosen system is minimal. In the chosen conditions, the size of the methanol box extending from the Cy3-ssDNA is 4.2 Å and from Cy3-dsDNA is 4.5 Å.

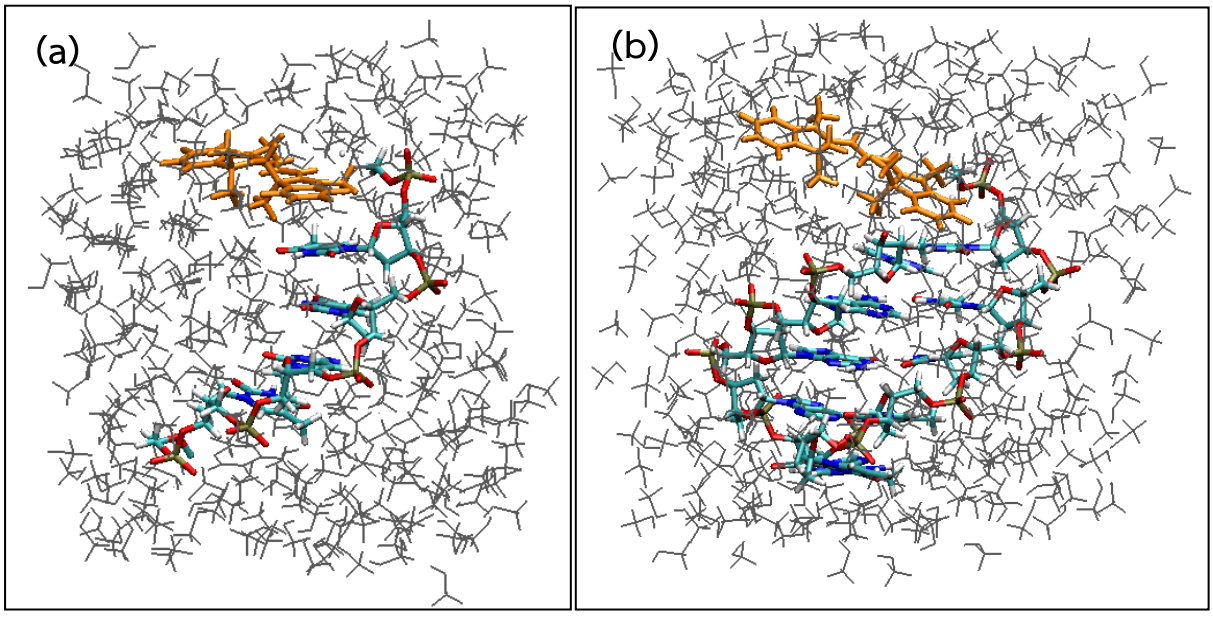

Figure 17. The optimized structure of Cy3-ssDNA (a) and Cy3-dsDNA (b) in methanol. The orange color represents Cy3. The methanol molecules are displays in gray color. For DNA strands, C, N, O, P and H atoms are in cyan, blue, red, tan and white colors, respectively.

4.6 The free energy of Cy3 obtained from 1-dimensional and 2-dimentional umbrella sampling

In case of 1-D umbrella sampling, the reaction coordinate is φ_2 which is fixed to 180^0, 170^0, ..., 70^0 in each window. From the simulations, the energy barriers for *trans-cis* isomerization are 1.6 kcal/mol for free-Cy3, 1.2 kcal/mol for Cy3-ssDNA and 3.4 kcal/mol for Cy3-dsDNA. The barrier peak in each case is located approximately in the range of 110^0 - 130^0 in accordance with the results from rigid torsion cuts. From the simulations, Cy3 attached to the double-stranded DNA has the highest activation energy while Cy3 attached to the single-stranded DNA has similar energy barrier to free-Cy3 (see **Figure 18** and **Table 4**). Although the results are contradictory to the experimental results of Cy3 that the energy barrier in the case of Cy3-ssDNA is higher than in Cy3-dsDNA,[2] these results are consistent with Cosa and coworkers' report on the fluorescence quantum yield of other cyanine dyes (PicoGreen, YOYO-1 iodide, SYBR Green I and SYBR Gold) bonded to the single- and double-stranded DNA.[3] From their observations, it was shown that the fluorescence quantum yield of the dye-dsDNA is higher than that of the dye-ssDNA. This indicates the larger energy barrier in the dye-dsDNA.[3]

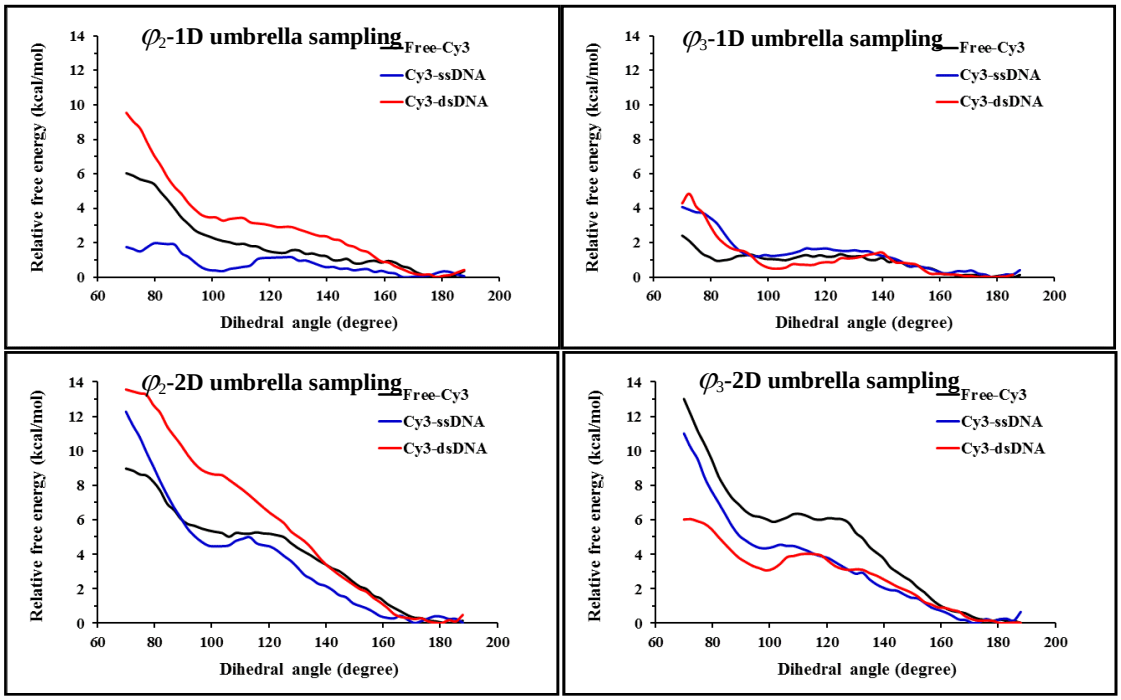

Figure 18. Relative free energy curves as a function of the dihedral angle for free-Cy3 (black), Cy3-ssDNA (blue) and Cy3-dsDNA (red). The free energy profiles from 1-D umbrella sampling for rotation of φ_2 and φ_3 are shown on the top panels, while the free energy from 2-D umbrella sampling for φ_2 and φ_3 are shown on the lower panels.

Table 4. Relative energies barrier as a function of the dihedral angle φ_2, φ_3 of 1-D umbrella sampling and 2-D umbrella sampling for Free-Cy3, Cy3-ssDNA and Cy3-dsDNA in kcal/mol.

Systems	Energies barrier for *trans-cis* isomerization (kcal/mol)			
	1D-umbrella sampling		2D-umbrella sampling	
	φ_2	φ_3	φ_2	φ_3
Free-Cy3	1.6*	1.2*	5.3*	6.1*
Cy3-ssDNA	1.2	1.7	5.0	4.6
Cy3-dsDNA	3.4	1.4	8.6	3.9

*Due the symmetry of the molecule in methanol, these barriers are interchangeable between φ_2 and φ_3.

The results of isomerization energy barriers obtained in this work can be explained by the influence of the Cy3-DNA interactions. Harvey et al. reported that the $\pi-\pi$ stacking interaction between Cy3 and nucleobases decreases the efficiency of photoisomerization and shows the increase in the energy barrier, both are correlated with increasing fluorescence efficiency and fluorescence lifetime.[4] In order to investigate such stacking interaction, the stacking distances between the atoms on the ring of terminal indole close to DNA and of T base of DNA primary strand are calculated (see **Figure 16** and **Figure 19**). It was found that on average, the stacking distances to the T base of the primary strand in Cy3-ssDNA are a little shorter than in Cy3-dsDNA. However, Cy3 is also at the same distance from the A base on the complementary strand (**Figure 19**). The stacking of Cy3 onto the double-stranded DNA seems to be a stable configuration as it is found in the NMR structure.[5] Therefore, the apparent higher isomerization barrier in the case of Cy3-dsDNA can be attributed to the stacking interaction. It can be seen that Cy3 has stacking interactions not only with the base in the primer strand but also with the base in the complementary strand. These interactions strengthen the stacking of Cy3 onto DNA bases, prevent the torsional rotation, and finally lead to the higher energy barrier. On the other hand, Cy3 stacked only to the T base on the primary strand in the Cy3-ssDNA case, implying weaker interaction and thus leading to the lower isomerization barrier. It can be inferred that an increase in the affinity between Cy3 and the strand of DNA causes the higher activation energy for isomerization. However, the different results between the simulations and the experiment[2] in the case of Cy3-ssDNA might come from the fact that there are various orientations of Cy3 relative to the ssDNA as well as dsDNA which are not covered in this report.

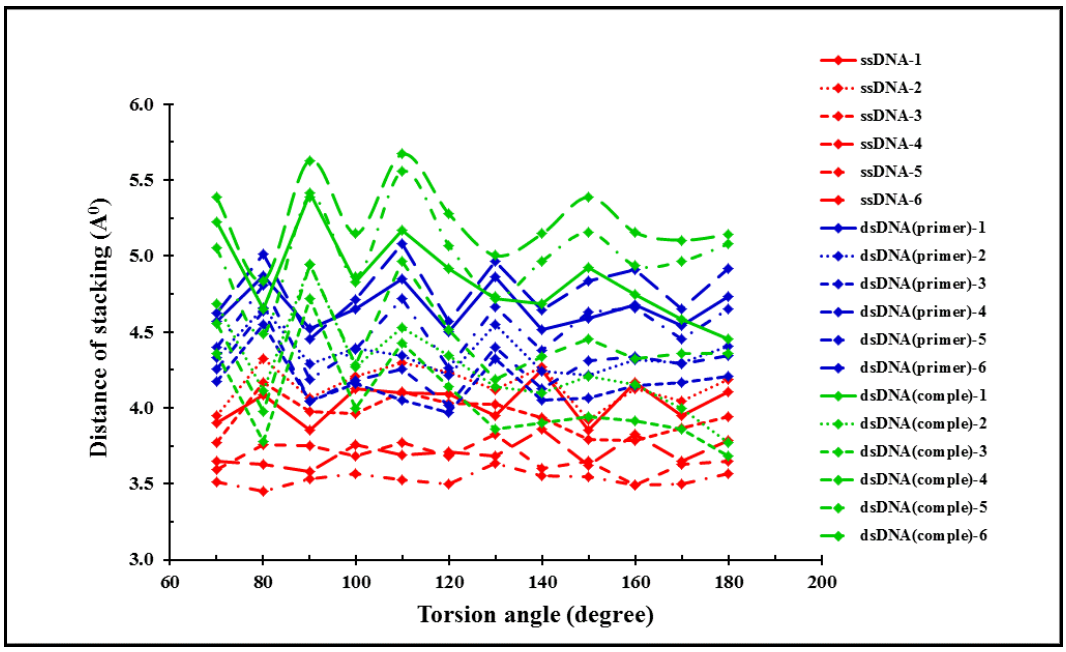

Figure 19. Stacking distances as a function of each dihedral angle (φ_2) from 1-D umbrella sampling. The distance at each dihedral angle is averaged from the 2 ps dynamics run in each window. The results from Cy3-ssDNA are in red, from Cy3-dsDNA (primer strand) are in blue and from Cy3-dsDNA (complementary strand) are in green. The indexes 1-6 are referred to **Figure 16**.

Moreover, Harvey et al. found that the enhancement of the fluorescence efficiency of Cy3 depends on the nucleobase type and is reflected by the energy barrier for isomerization, i.e., the barrier when Cy3 attached to the purine (A, G) is larger than when it is attached to the pyrimidine (C, T).[4] In their experiment, the activation energy when Cy3 is attached to guanine is highest (7.0 $\pm$ 0.1 kcal/mol) whereas when it is attached to thymine, the barrier is lowest (5.2 kcal/mol).[4] It agrees with our preliminary results as when the initial base is changed from thymine to guanine, the activation energy for isomerization of φ_2 increases to 2.7 kcal/mol from 1.2 kcal/mol in the case of Cy3 attached to the single-stranded DNA and to 4.9 kcal/mol from 3.4 kcal/mol in the case of Cy3 attached to the double-stranded DNA. It is also consistent with Spiriti et al.'s results that the affinity of Cy3 attached to the 5′ end of the double-stranded DNA (Cy3 stacking on T base) is shown to be significantly less than the case of other basepairs.[6] These results highlight the

significant role of stacking interactions between Cy3 and DNA in its photophysical properties.

For the rotation of dihedral angle φ_3 of Cy3-dsDNA, the energy barrier obtained from 1-D umbrella sampling is lower than for φ_2. In the case of Cy3-ssDNA, the energy barriers of the two angles are similar. These results are related to the steric effect, and will be discussed in the next section.

In 1-D umbrella sampling, for all conditions of Cy3, it was found that when φ_2 is constrained, φ_4 also twists and Cy3 becomes non-planar as indicated from the four torsion angles during the course of dynamics shown in **Figure 20.** Likewise, when φ_3 is constrained, it makes φ_1 twists and the dye structure is non-planar as shown in **Figure 21**. To distinguish the effect of the rotation of one bond at a time, the 2-D umbrella sampling is employed. In 2-D umbrella sampling the main reaction coordinate is the dihedral angle φ_2 like in 1-D case. The additional reaction coordinate is φ_4, which is constrained to 180^0 to maintain the planarity of Cy3 in all varying windows of φ_2. Likewise, for the free energy calculation of primary reaction coordinate φ_3, the second constraint is the dihedral angle φ_1, which is constrained to 180^0.

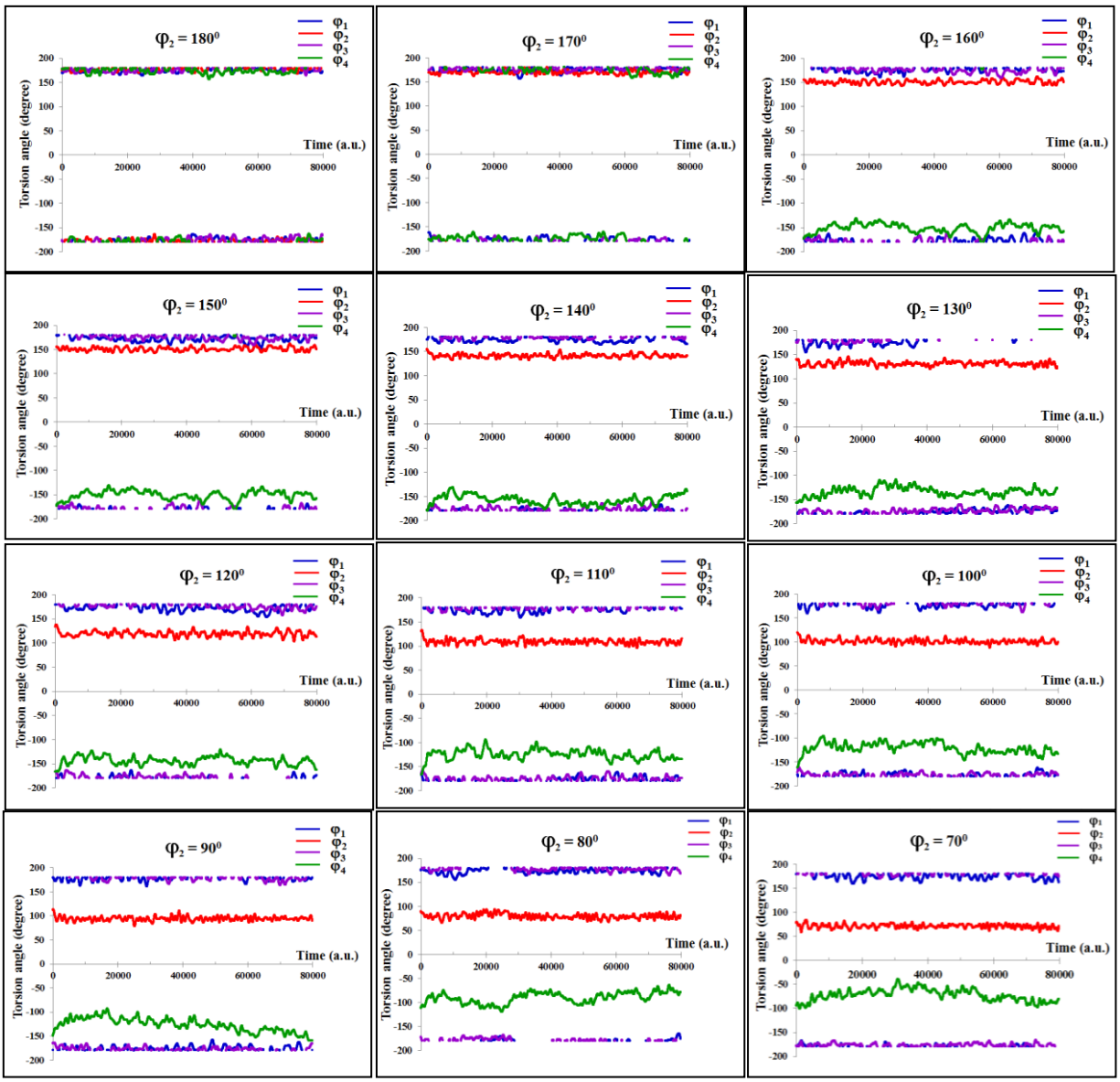

Figure 20. The dihedral angles of each bond on the trimethine chain of Cy3-ssDNA from 1-D umbrella sampling. The reaction coordinate is the dihedral angle φ_2. The colors displayed for φ_1 is dark blue, for φ_2 is red, for φ_3 is purple and for φ_4 is green. Notice that φ_4 is more deviated from planarity (180^0) when φ_2 is more twisted starting from 130^0 toward 70^0.

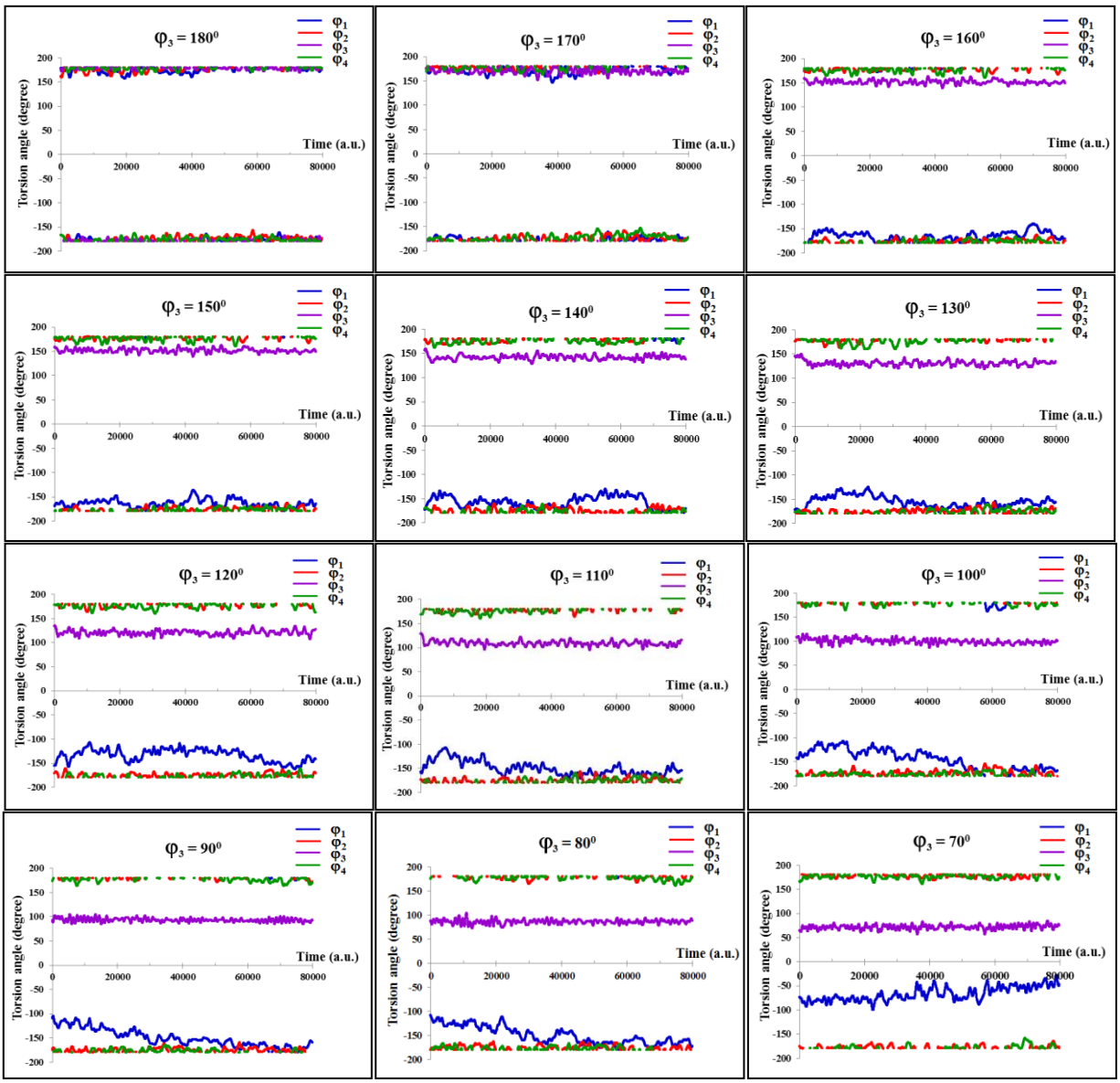

Figure 21. The dihedral angles of each bond on the trimethine chain of Cy3-ssDNA from 1-D umbrella sampling. The reaction coordinate is the dihedral angle φ_3. The colors displayed for φ_1 is dark blue, for φ_2 is red, for φ_3 is purple and for φ_4 is green. Notice that φ_1 is more deviated from planarity (180^0) when φ_3 is more twisted starting from 130^0 toward 70^0.

As shown in **Table 4**, the trend of activation energy for *trans-cis* isomerization of all systems in 2-D umbrella sampling is very similar to 1-D umbrella sampling, but with two- to five-fold increase in the barrier upon constraining the terminal dihedral angle (φ_1 or φ_4) to 180^0. This suggests that the photophysics of Cy3

is influenced by more than one dihedral angle along the conjugated bridge. When φ_4 is constrained to 180^0, it will affect the rotation of φ_2 and leads to an increased energy barrier for *trans-cis* isomerization. For the rotation of dihedral angle φ_2, the activation energy of Cy3-dsDNA is significantly higher than in the case of free-Cy3 and Cy3-ssDNA, which share similar values as shown in **Table 4**. These results can be explained by the stacking interaction of Cy3 not only with the base in the primer strand but also with the one in the complementary strand as discussed above. The stacking distances of Cy3-ssDNA and Cy3-dsDNA in the case of 2-D umbrella sampling are shown in **Figure 22**. It was found that on average, the stacking distances in Cy3-ssDNA are a bit shorter than in Cy3-dsDNA. However, Cy3 has stacking interactions with the first base on both the primary and complementary strands. This again shows that Cy3 is more rigidified when it is bonded to ds-DNA due to the additional stacking interactions with the base on the complementary strand. Therefore, it leads to the higher barrier for isomerization of φ_2.

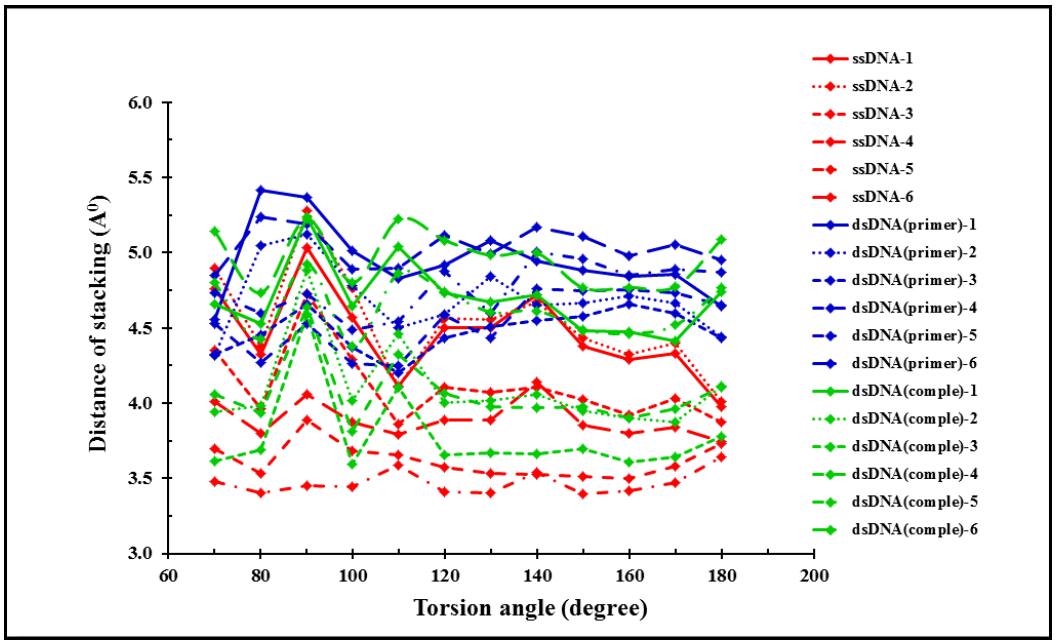

Figure 22. Stacking distances as functions of each dihedral angle (φ_2) from 2-D umbrella sampling. The distance at each dihedral angle is averaged from the 2 ps dynamics run in each window. The results from Cy3-ssDNA are in red, Cy3-dsDNA (primer strand) are in blue and Cy3-dsDNA (complementary strand) are in green. The indexes 1-6 are referred from **Figure 16**.

For the rotation of the dihedral angle φ_3, the energy barriers for isomerization obtained from three conditions (free, ssDNA bound and dsDNA bound) are quite similar in both 1-D and 2-D umbrella samplings. Interestingly in case of 1-D umbrella sampling of Cy3-dsDNA, the energy barrier for the rotation of φ_3 is distinguishably lower than the one of φ_2. This is also observed in the case of 2-D umbrella sampling. This result is hypothesized to be attributed to the steric hindrance. From the simulations, while φ_2 or φ_3 are rotating, the structure on the right side (connected to the DNA) of the rotated bond is constrained as can be seen in **Figure 19** and **Figure 22** that the average distance between the phenyl ring on the right indole group of Cy3 and the first base of the primary strand of DNA does not change significantly. As shown in **Figure 23**, when Cy3 is twisted the right side of Cy3 only moves slightly, which might be due to the fact that it is attached to the bulky DNA. On the other hand, the left side undergoes more movement as a result of the torsional rotation. When the dihedral angle φ_2 is rotated, the left side of Cy3 moves downward (**Figure 23(a)**). On the other hand, when the dihedral angle φ_3 is rotated, the left side of the molecule moves upward (**Figure 23(b)**). Therefore, it can be inferred that the part that plays a more important role in the isomerization barrier is the left side of Cy3.

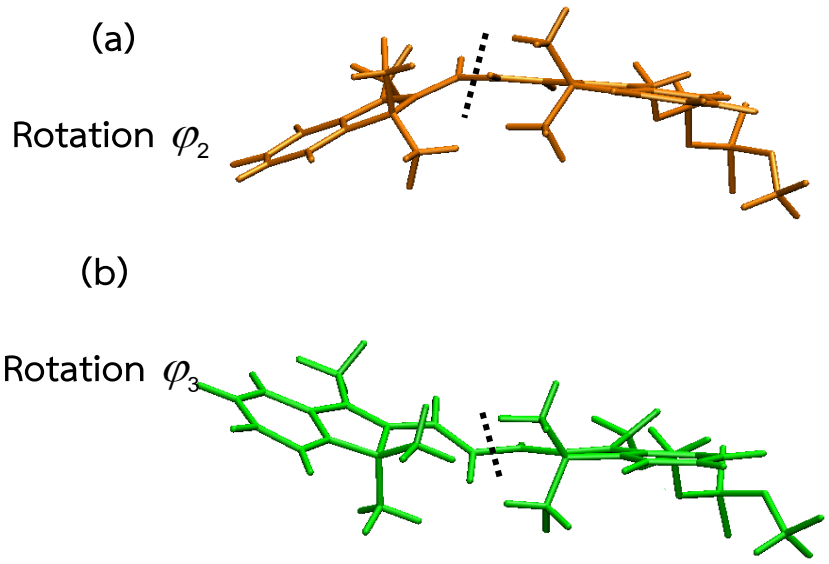

Figure 23. The structure at 90^0 rotation of each dihedral angle belonging to the trimethine chain of Cy3 from Cy3-dsDNA 2-D umbrella sampling. The right side of Cy3 is bonded to the DNA strand. In (a) the dihedral angle φ_2 is rotated and the left side of Cy3 moves down. In (b) the dihedral angle φ_3 is rotated and the left side of the molecule moves up. Dotted lines divide Cy3 to the left and right of the rotating angle.

To prove the hypothesis about the steric effect, the distances between the nitrogen atoms of the first A base on the complementary strand and the methylic carbon atoms on the left side of Cy3, further away from the primary strand, as shown in **Figure 24**, are calculated. As illustrated in **Figure 25(a)** and **(b)**, when φ_2 is rotated (dotted lines) the N_i-C_i distances is considerably shorter than when φ_3 is rotated (solid lines), especially when the dihedral angles are below 160°. These results are consistent to Park and coworkers' study that the steric hindrance is associated with the rotation of the bond composed of heavy atoms, i.e., the C-C bonds in polymethine chain and such hindrance can affect the energy barrier for *trans-cis* isomerization.[7] This result obtained here infers that in the case of φ_2 rotation, there is more steric hindrance and thus it leads to an increase in the energy barrier of φ_2 compare to φ_3. This explanation can be similarly applied in case of the rotation of φ_3 in Cy3-dsDNA from 1-D umbrella sampling as well.

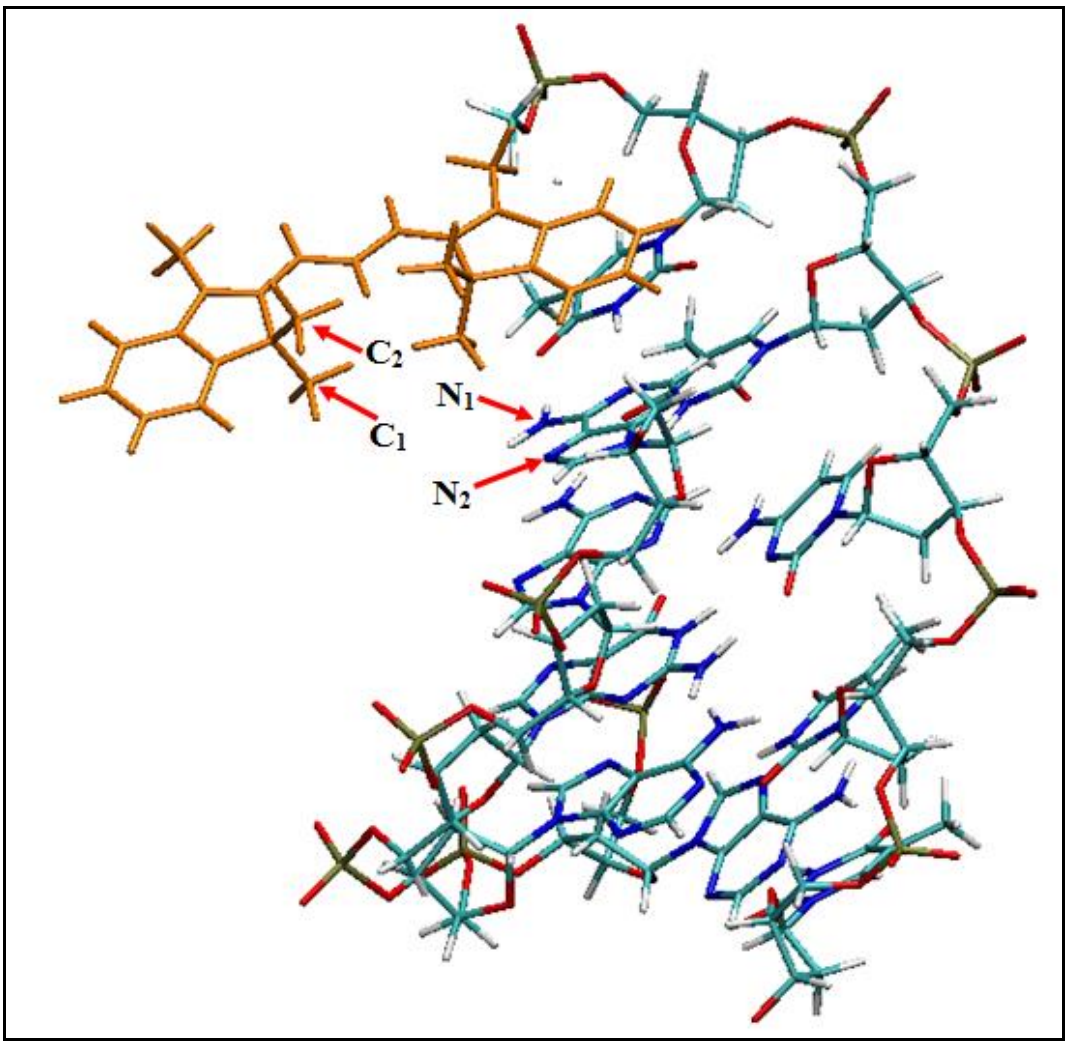

Figure 24. The indexes of atom used in the calculations of the distances between the nitrogen atoms of the first base on the DNA complementary strand and the carbon atoms of the methyl groups of Cy3 (orange color) on the left side (far from the DNA primary strand).

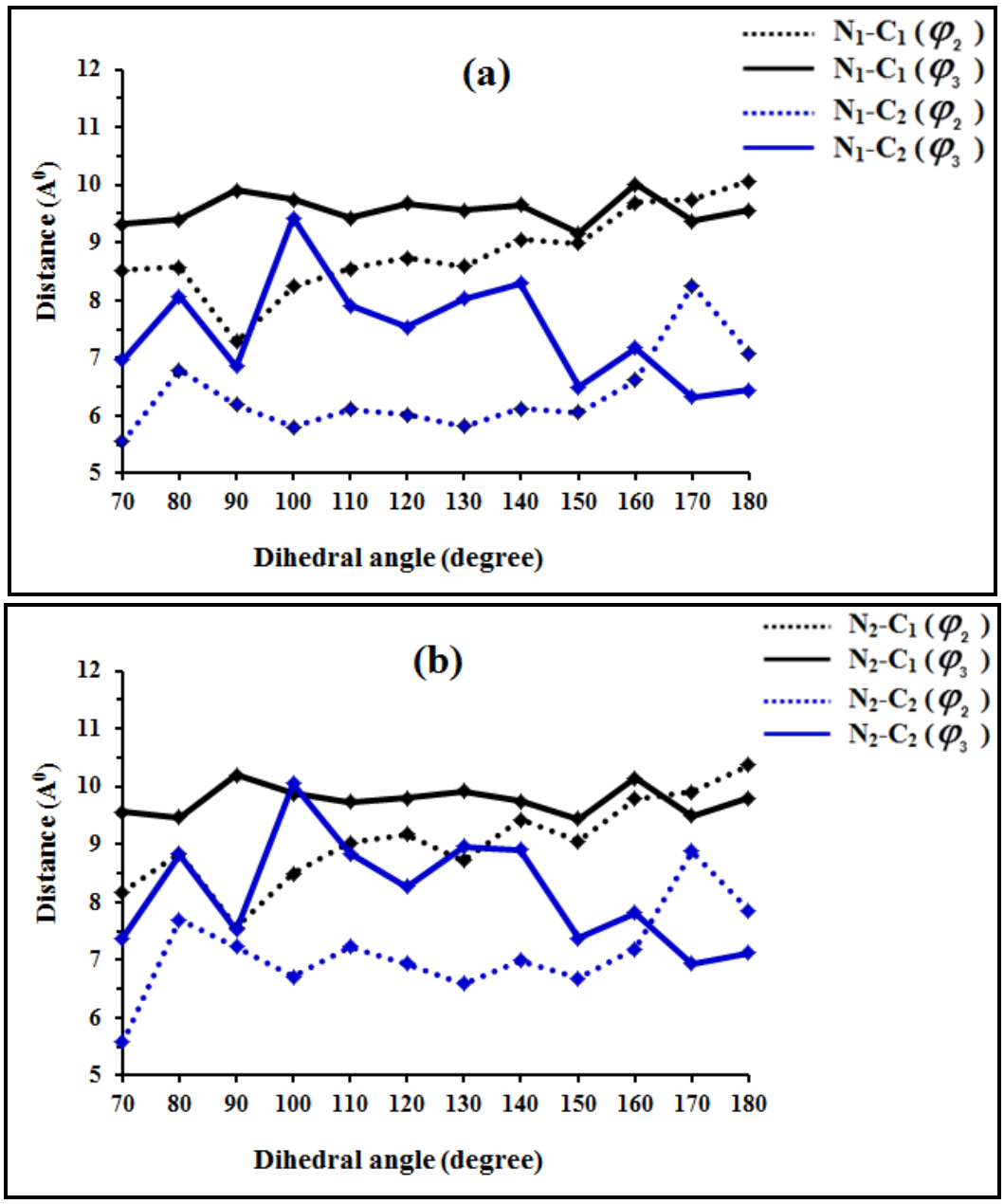

Figure 25. The top panel (a) shows the distances between the nitrogen atom (N_1) of the first base on the DNA complementary strand and the carbon atoms (C_1 and C_2) of the methyl groups of Cy3 on the left (far from the primary strand). The lower panel (b) shows the distance between the nitrogen atom (N_2) of the first base on the complementary strand of DNA and the carbon atoms (C_1 and C_2) of the same Cy3 methyl groups on the left. The dotted lines represent the distances when the dihedral angle φ_2 is rotated while the solid lines represent the distances when φ_3 is rotated. These results are averaged from 2 ps duration of each window of dihedral angle in Cy3-dsDNA 2D-umbrella sampling.

CHAPTER 5

CONCLUSION

The photophysical properties of the symmetrical cyanine dye Cy3 when being free or attached to the single- and double-stranded DNA are studied by using QM/MM dynamics simulations with umbrella sampling technique and WHAM for free energy calculations. From this investigation, it is indicated that the environment of Cy3 is important in its fluorescence applications and can lead to differences in the photophysical properties in accordance with the experimental results. *Trans-cis* isomerization is the main nonradiative process that competes with the radiative fluorescence deactivation from the excited state. The activation energy for *trans-cis* isomerization is highest when Cy3 is attached to the double-stranded DNA because the structure of the dye is most rigidified due to the stacking interaction. Thus, Cy3-dsDNA is deactivated more efficiently by fluorescence than *trans-cis* isomerization. Furthermore, the type of DNA base can also influence the stacking interaction which can also affect the photophysics of Cy3. If Cy3 is attached to the thymine (T) base of DNA rather than guanine (G), it shows the low energy barrier for *trans-cis* isomerization, thus decreasing the fluorescence efficiency. Moreover, the steric hindrance is associated with the rotation around the conjugated bonds of Cy3. If Cy3 has high steric hindrance, it shows the high energy barrier for the rotation, thus increasing the efficiency of fluorescence.

References

(1) Ma, X.; Hua, J.; Wu, W.; Jin, Y.; Meng, F.; Zhan, W.; Tian, H.: A high-efficiency cyanine dye for dye-sensitized solar cells. Tetrahedron. 2008, 64, 345-350.

(2) Weissberger, A.; Taylor, E. C.: The chemistry of heteroaromatic compounds. In Synthesis and properties - cyanine and related dyes; Sturmer, D. M., Ed.; Wiley: New York, 1977; Vol. 30.

(3) Sanborn, M. E.; Connolly, B. K.; Gurunathan, K.; Levitus, M.: Fluorescence Properties and Photophysics of the Sulfoindocyanine Cy3 Linked Covalently to DNA. J. Phys. Chem. 2007, 111, 11064-11074.

(4) Schaberle, F. A.; Kuz'min, V. A.; Borissevitch, I. E.: Spectroscopic studies of the interaction of bichromophoric cyanine dyes with DNA. Effect of ionic strength. Biochimica et Biophysica Acta (BBA). 2003, 1621, 183-191.

(5) Kabatc, J.; Pączkowski, J.: The photophysical and photochemical properties of the oxacarbocyanine and thiacarbocyanine dyes. Dyes Pigments. 2004, 61, 1-16.

(6) Armitage, B. A.: Cyanine Dye–DNA Interactions: Intercalation, Groove Binding, and Aggregation. Springer-Verlag. 2005, 253, 55-76.

(7) Armitage, B. A.: Cyanine Dye–Nucleic Acid Interactions. Springer-Verlag. 2008, 14, 11-29.

(8) Wei, L.; XuDong, C.; Damir, A.; AnDong, X.: Single molecule fluorescence fluctuations of the cyanine dyes linked covalently to DNA. Sci China Ser B-Chem. 2009, 52, 1148-1153.

(9) Ernst, L. A.; Gupta, R. K.; Mujumdar, R. B.; Waggoner, A. S.: Cyanine Dye Labeling Reagents for Sulfhydryl Groups. Cytometry 1989, 10, 3-10.

(10) Silva, G. L.; Ediz, V.; Yaron, D.; Armitage, B. A.: Experimental and Computational Investigation of Unsymmetrical Cyanine Dyes: Understanding Torsionally Responsive Fluorogenic Dyes. J. Am. Chem. Soc. 2007, 129, 5710-5718.

(11) Mishra, A.; Behera, R. K.; Behera, P. K.; Mishra, B. K.; Behera, G. B.: Cyanines during the 1990s: A Review Chem. Rev. 2000, 100, 1973–2011.

(12) Kim, E.; Park, S. B.: Advanced Fluorescence Reporters in Chemistry and Biology I: Fundamentals and Molecular Design; Springer Ser Fluoresc, 2010; Vol. 8.

(13) Mojzych, M.; Henary, M.: Synthesis of Cyanine Dyes; Springer-Verlag.: Berlin Heidelberg, 2008; Vol. 14.

(14) Russell, S.; Meadows, L. A.; Russell, R. R.: Microarray Technology in Practice; Elsevier Inc.: USA, 2009.

(15) Jia, K.; Wan, Y.; Xia, A.; Li, S.; Gong, F.; Yang, G.: Characterization of Photoinduced Isomerization and Intersystem Crossing of the Cyanine Dye Cy3. J. Phys. Chem. 2007, 111, 1593-1597.

(16) Sauer, M.; Hofkens, J.; Enderlein, J.: Handbook of Fluorescence Spectroscopy and Imaging; WILEY-VCH.: Weinheim, Germany, 2011.

(17) Valeur, B.: Molecular Fluorescence: Principles and Applications; Wiley-VCH., 2002.

(18) Cosa, G.; Focsaneanu., K. S.; McLean., J. R. N.; McNamee., J. P.; Scaiano., J. C.: Photophysical Properties of Fluorescent DNA-dyes Bound to Single- and Double-stranded DNA in Aqueous Buffered Solution. Photochem. Photobiol. 2001, 73, 585-599.

(19) Harvey, J. B.; Levitus, M.: Nucleobase-Specific Enhancement of Cy3 Fluorescence. J. Fluoresc. 2009, 19, 443-448.

(20) Malicka, J.; Gryczynski., I.; Maliwai., B. P.; Fang., J.; Lakowicz., J. R.: Fluorescence spectral properties of cyanine dye labeled DNA near metallic silver particles. Biopolymers. 2003, 72, 96-104.

(21) Norman, D. G.; Grainger., R. J.; Uhrı́n., D.; Lilley., D. M. J.: Location of cyanine-3 on double-stranded DNA: Importance for fluorescence resonance energy transfer studies. Biochemistry 2000, 39, 6317-6324.

(22) Ouellet, J.; Schorr., S.; Iqbal., A.; Wilson., T. J.; Lilley., D. M. J.: Orientation of cyanine fluorophores terminally attached to DNA via long, flexible tethers. Biophys. J. 2011, 101, 1148-1154.

(23) Mark, B.; Timothy, R. B.; Zhuang, X. W.: Short-Range Spectroscopic Ruler Based on a Single-Molecule Optical Switch. Phys. ReV. Lett. 2005, 94, 108101.

(24) KÖhn, F.; Hofkens, J.; Gronheid, R.; Auweraer, M. V.; Schryver, F. C. D.: Parameters Influencing the On- and Off-Times in the Fluorescence Intensity Traces of Single Cyanine Dye Molecules. J. Phys. Chem. A. 2002, 106, 4808-4814.

(25) Obliosca, J. M.; Wang., P.; Tseng., F.: Probing quenched dye fluorescence of Cy3–DNA–Au-nanoparticle hybrid conjugates using solution and array platforms. J. Colloid Interface Sci. 2012, 371, 34-41.

(26) Hunt, P. A.; Robb, M. A.: Systematic Control of Photochemistry: The Dynamics of Photoisomerization of a Model Cyanine Dye. J. Am. Chem. Soc. 2005, 127, 5720-5726.

(27) Vaveliuk, P.; Scaffardi, L. B.; Duchowicz, R.: Kinetic Analysis of a Double Photoisomerization of the DTDCI Cyanine Dye. J. Phys. Chem. 1996, 100, 11630-11635.

(28) Rulliere, C.: Laser action and photoisomerization of 3,3'-diethyl oxadicarbocyanine iodide (dodci) -influence of temperature and concentration. Chem. Phys. Lett. 1976, 43, 303-308.

(29) Ponterini, G.; Momicchioli, F.: Trans cis photoisomerization mechanism of carbocyanines - experimental check of theoretical-models. Chem. Phys. 1991, 151, 111-126.

(30) Momicchioli, F.; Baraldi., I.; Bertheir., G.: Theoretical-study of trans cis photoisomerism in polymethine cyanines. Chem. Phys. 1988, 123, 103-112.

(31) Cao, J.; Wu, T.; Hu, C.; Liu, T.; Sun, W.; Fan, J.; Peng, X.: The nature of the different environmental sensitivity of symmetrical and unsymmetrical cyanine dyes: an experimental and theoretical study. Phys. Chem. Chem. Phys. 2012, 14, 13702-13708.

(32) Nygren, J.; Svanvik., N.; Kubista., M.: The Interactions Between the Fluorescent Dye Thiazole Orange and DNA. Biopolymers. 1998, 46, 39-51.

(33) Brismar, H.; Trepte., O.; Ulfhake., B.: Spectra and fluorescence lifetimes of lissamine rhodamine, tetramethylrhodamine isothiocyanate, texas red,

and cyanine-3.18 fluorophores: influences of some environmental factors recorded with a confocal laserscanning microscope. J. Histochem. Cytochem. 1995, 43, 699–707.

(34) Lee, H.; Y., B. M.; Henary, M.; Strekowski, L.; Achilefu, S.: Fluorescence lifetime properties of near-infrared cyanine dyes in relation to their structures. J. Photochem. Photobiol., A 2008, 200, 438-444.

(35) Spiriti, J.; Binder, J. K.; Levitus, M.; Vaart, A.: Cy3-DNA Stacking Interactions Strongly Depend on the Identity of the Terminal Basepair. Biophys. J. 2011, 100, 1049-1057.

(36) Sanchez-Galvez, A.; Hunt., P.; Robb., M. A.; Olivucci., M.; Vreven., T.; Schlegel., H. B.: Ultrafast Radiationless Deactivation of Organic Dyes: Evidence for a Two-State Two-Mode Pathway in Polymethine Cyanines. J. Am. Chem. Soc. 2000, 122, 2911-2924.

(37) Park, J.: AM1 semiempirical calculated potential energy surfaces for the isomerization of symmetrical carbocyanines. Dyes Pigments. 2000, 46, 155-161.

(38) Warshel, A.; Levitt, M.: Theoretical Studies of Enzymic Reactions : Dielectric, Electrostatic and Steric Stabilization of the Carbonium Ion in the Reaction of Lysozyme. J. Mol. Biol. 1976, 103, 227-249.

(39) Levitus, M.; Ranjit., S.: Cyanine dyes in biophysical research: the photophysics of polymethine fluorescent dyes in biomolecular environments. Quarterly Reviews of Biophysics 2011 44, 123-151.

(40) Jorgensen, W. L.; Maxwell, D. S.; Tirado-Rives, J.: Development and Testing of the OPLS All-Atom Force Field on Conformational Energetics and Properties of Organic Liquids. J. Am. Chem. Soc. 1996, 118, 11225-11236.

(41) Case, D. A.; Pearlman, D. A.; Caldwell, J. W.; III, T. E. C.; Wang, J.; Ross, W. S.; Simmerling, C. L.; Darden, T. A.; Merz, K. M.; Stanton, R. V.; Cheng, A. L.; Vincent, J. J.; Crow-ley, M.; Tsui, V.; Gohlke, H.; Radmer, R. J.; Duan, Y.; Pitera, J.; , J.; Massova, I.; Seibel, G. L.; Singh, U. C.; Weiner, P. K.; Kollman, P. A.: AMBER 7: University of California: San Francisco, CA, USA, 2002.

(42) Cornell, W.; Cieplak, P.; Bayly, C.; Gould, I.; Merz, J. K.; Ferguson, D.; Spellmeyer, D.; Fox, T.; Caldwell, J.; Kollman, P.: A Second Generation Force Field for the Simulation of Proteins, Nucleic Acids, and Organic Molecules. J. Am. Chem. Soc. 1995, 117, 5179-5197.

(43) Kollman, P. A.; Weiner, P. K.: AMBER: Assisted model building with energy refinement. A general program for modeling molecules and their interactions. J. Comput. Chem. 1981, 2, 287-303.

(44) Weiner, S. J.; Kollman, P. A.; Case, D. A.; Singh, U. C.; Ghioand, C.; Alagona, G.; Jr., S. P.; Weiner, P.: A New Force Field for Molecular Mechanical Simulation of Nucleic Acids and Proteins. J. Am. Chem. Soc. 1984, 106, 765-784.

(45) Granucci, G.; Toniolo., A.: Molecular gradients for semiempirical CI wavefunctions with floating occupation molecular orbitals. Chem. Phys. Lett. 2000, 32, 79-85.

(46) Roos, B. O.: The Complete Active Space Self-Consistent Field Method and its Applications in Electronic Structure Calculations. Adv. Chem. Phys. 1987, 69, 399.

(47) Stewart, J. J. P.: MOPAC 2000; Fujitsu Limited: Tokyo, Japan, 1999.

(48) Owens, J. M.: Theoretical Studies of the Solvation, Dynamics, and Photochemistry of Ethylene, Retinal Protonated Schiff Base, Oligocellulose, and GD(III) Clusters. University of Illinois at Urbana-Champaign, Urbana, 2004.

(49) Ben-num, N.; Martínez, T. J.: Ab initio quantum molecular dynamics. Adv. Chem. Phys. 2002, 121, 439.

(50) Ben-Nun, M.; Quenneville, J.; Martínez, T. J.: Ab Initio Multiple Spawning: Photochemistry from First Principles Quantum Molecular Dynamics. J. Phys. Chem. A 2000, 104A, 5161.

(51) Werner, H. J.; Knowles, P. J.; Lindh, R.; Schuetz, M.; Celani, P.; Korona, T.; Manby, F. R.; Rauhut, G.; Amos, R. D.; Bernhardsson, A.; Berning, A.; Cooper, D. L.; Deegan, M. J. O.; Dobbyn, A. J.; Eckert, F.; Hampel, C.; Hetzer, G.; Lloyd, A. W.; McNicholas, S. J.; Meyer, W.; Mura, M. E.; Nicklass, A.; Palmieri, P.; Pitzer, R.;

Schumann, U.; Stoll, H.; Stone, A. J.; Tarroni, R.; Thorsteinsson, T.: MOLPRO, 2006.1. 2006.

(52) Torrie, G. M.; Valleau, J. P.: Non-Physical Sampling Distributions in Monte-Carlo Free-Energy Estimation - Umbrella Sampling. J. Comput. Phys. 1977, 23, 187-199.

(53) Kumar, S.; Djamal, B.; Robert, S.; P.Kollmana; Rosenbergl, J.: The Weighted Histogram Analysis Method for Free-Energy Calculations on Biomolecules. I. The Method. J. Comput. Chem. 1992, 13, 1011-1021.

(54) F., W. S.; Zhou, T.; Huang, Y. C.; Ye, S. Y.: DFT Investigation on the Trans-cis Photoisomerization of Pentamethine Cyanine Dye Model Molecule. Chinese J. Struct. Chem. 2011, 30, 401-411.

(55) Rodríguez, J.; Scherlis, D.; Estrin, D.; Aramendía, P. F.; Negri, R. M.: AM1 Study of the Ground and Excited State Potential Energy Surfaces of Symmetric Carbocyanines. J. Phys. Chem. A. 1997, 101, 6998-7006.

(56) Humphrey, W.; Dalke, A.; Schulten, K.: VMD: Visual Molecular Dynamics. J. Mol. Graph. 1996, 14, 33-38.

(57) Iqbal, A.; Wang, L.; Thompson, K. C.; Lilley, D. M. J.; Norman, D. G.: The Structure of Cyanine 5 Terminally Attached to Double-Stranded DNA:Implications for FRET Studies. Biochemistry 2008, 47, 7857–7862.

VITAE

Name Miss Pilailuk Sawangsang

Student ID 5310220046

Educational attainment

Degree	Name of Institution	Year of Graduation
Degree of Bachelor of Science in Physics	Prince of Songkla University	2007
Graduate Diploma (Teaching Profession)	Silpakorn University	2008

Scholarship

1. Graduate School Research Support Funding for Thesis (2010-2011) from the graduate school, Prince of Songkla University.
2. Research Assistant from the faculty of science, Prince of Songkla University.